Interactive Initialization and Continuation of Homoclinic and Heteroclinic Orbits in MATLAB

VIRGINIE DE WITTE and WILLY GOVAERTS, Ghent University
YURI A. KUZNETSOV, Utrecht University
MARK FRIEDMAN, University of Alabama, Huntsville

MATCONT is a MATLAB continuation package for the interactive numerical study of a range of parameterized nonlinear dynamical systems, in particular ODEs, that allows to compute curves of equilibria, limit points, Hopf points, limit cycles, flip, fold and torus bifurcation points of limit cycles. It is now possible to continue homoclinic-to-hyperbolic-saddle and homoclinic-to-saddle-node orbits in MATCONT. The implementation is done using the continuation of invariant subspaces, with the Riccati equations included in the defining system. A key feature is the possibility to initiate both types of homoclinic orbits interactively, starting from an equilibrium point and using a homotopy method. All known codimension-two homoclinic bifurcations are tested for during continuation. The test functions for inclination-flip bifurcations are implemented in a new and more efficient way. Heteroclinic orbits can now also be continued and an analogous homotopy method can be used for the initialization.

Categories and Subject Descriptors: G.1.0 [**Numerical Analysis**]: General—*Numerical algorithms*; G.4 [**Mathematical Software**]: *Algorithm design and analysis*; J.2 [**Physical Sciences and Engineering**]: *Mathematics and statistics*

General Terms: Algorithms, Theory

Additional Key Words and Phrases: Global bifurcation, numerical continuation, homotopy

ACM Reference Format:
De Witte, V., Govaerts, W., Kuznetsov, Y. A., and Friedman, M. 2012. Interactive initialization and continuation of homoclinic and heteroclinic orbits in MATLAB. ACM Trans. Math. Softw. 38, 3, Article 18 (April 2012), 34 pages.
DOI = 10.1145/2168773.2168776 http://doi.acm.org/10.1145/2168773.2168776

1. INTRODUCTION

A continuous-time dynamical system is usually defined by a set of ordinary differential equations (ODEs)

$$\dot{x} = f(x, \alpha), \tag{1}$$

where $x \in \mathbb{R}^n$ is a state vector, $\alpha \in \mathbb{R}^p$ is a parameter vector and $f : \mathbb{R}^n \times \mathbb{R}^p \to \mathbb{R}^n$ is a smooth function. For general background on dynamical systems theory we refer to

M. Friedman was supported in part under NSF DMS-0209536 and NSF ATM-0417774.
Authors' addresses: V. De Witte and W. Govaerts, Department of Applied Mathematics and Computer Science, Ghent University, Krijgslaan 281-S9, 9000 Gent, Belgium; email: {Virginie.DeWitte, Willy.Govaerts}@UGent.be; Y. A. Kuznetsov, Department of Mathematics, Utrecht University, Budapestlaan 6, 3584 CD Utrecht, The Netherlands; email: I.A.Kouznetsov@uu.nl; M. Friedman, Mathematical Sciences Department, University of Alabama, Huntsville, 201N SC, Huntsville, AL 35899; email: Friedman@math.uah.edu.

DOI 10.1145/2168773.2168776 http://doi.acm.org/10.1145/2168773.2168776

the existing literature, in particular, Guckenheimer and Holmes [1983] and Kuznetsov [2004].

MATCONT [Dhooge et al. 2003] is an interactive MATLAB package for the study of dynamical systems and their bifurcations. Among other things, it supports the numerical continuation of equilibria, limit cycles, saddle-node and Hopf bifurcations of equilibria, and fold, period-doubling, and torus bifurcations of limit cycles, as well as their normal form analysis. The package is freely available at `http://sourceforge.net/projects/matcont`. MATCONT is a successor package to AUTO [Doedel et al. 1997a] and CONTENT [Kuznetsov and Levitin 1998], which are written in compiled languages (Fortran, `C`, `C++`). The MATLAB platform of MATCONT is attractive because it is user-friendly, portable to all operating systems, and allows a standard handling of data files, graphical output and so on. While performing individual numerical tasks slower than the compiled-language packages, it usually saves time if the total man-machine time needed to study an ODE system is taken into account.

In dynamical systems theory, an orbit corresponding to a solution $x(t)$ is called homoclinic to the equilibrium point x_0 of (1) if $x(t) \to x_0$ as $t \to \pm\infty$. There are two types of such homoclinic orbits with codimension 1, namely homoclinic-to-hyperbolic-saddle (HHS) orbits, if x_0 is a hyperbolic saddle, and homoclinic-to-saddle-node (HSN) orbits, if x_0 is a saddle-node. Codimension 1 means that in generic dynamical systems with two free parameters ($p = 2$) these orbits exist along curves in the parameter plane. Both types of homoclinic orbits are important in numerous applications, for example, as wave solutions in combustion models [Berestycki and Nirenberg 1992], to model "excitation" in models of biological cells [Rinzel and Ermentrout 1989], chemical reactions [Gray and Scott 1990], etc. Hetroclinic orbits correspond to solutions of (1) with $x(t) \to x_{0,1}$ as $t \to \pm\infty$, where equilibria x_0 and x_1 are distinct. Heteroclinic orbits connecting hyperbolic equilibria can have codimension 0 (i.e., persist under parameter variations) or higher; they are also important in applications.

The first efficient methods for continuation of homoclinic or heteroclinic orbits to equilibria have been developed and implemented as HomCont toolbox in the standard software AUTO97, see Doedel and Friedman [1989], Beyn [1990], Champneys and Kuznetsov [1994], and Champneys et al. [1996]. These methods are based on the truncated boundary value problems (BVPs) with projection boundary conditions and integral phase conditions, which are then discretized using piecewise-polynomial approximation with orthogonal collocation. Starting from the same basic ideas, we present in this paper new or improved algorithms for the numerical continuation of connecting (i.e., homoclinic or heteroclinic) orbits and the first fully interactive implementation of these algorithms, in MATCONT. The resulting tool combines various ingredients from Champneys et al. [1996], Champneys and Kuznetsov [1994], Demmel et al. [2000], and Bindel et al. [2008], but differs from any existing implementation and contains several new interactively supported functionalities not available elsewhere, as is explained below.

There are essential differences between HomCont and our implementation. HomCont employs a technique due to Beyn [1990] to ensure the smoothness of the bases in the generalized eigenspaces used in the projection boundary conditions. These bases are originally computed in each step by black-box linear algebra routines. As a consequence – also in the latest AUTO-versions – some blocks of the Jacobian matrix of the discretized projection BVP are approximated by finite differences, even if all partial derivatives of the right-hand side of (1) with respect to (x, α) are provided by the user. Our construction of the projection boundary conditions is different and is based on the "Continuation of Invariant Subspaces" algorithm [Dieci and Friedman

2001], where the Riccati equations play the central role. However, unlike Demmel et al. [2000], we include the Riccati equations in the defining truncated BVP. This allows us to set up the Jacobian matrix of the discretized defining system avoiding finite differences, if the user-supplied derivatives are available. In this way we simultaneously continue the connecting solution and the (orthogonal complements to) stable and unstable invariant subspaces of $f_x(x_0, \alpha)$, which makes the continuation more robust.

In this article we also give test functions for the detection of a large number of codimension 2 bifurcations, which are checked for during the continuation of homoclinic orbits. HomCont also detects these codim 2 homoclinic bifurcations. However, in MATCONT, test functions for the inclination-flip bifurcations are implemented in a new and more efficient way (HomCont uses a system with double size). Moreover, in MATCONT, no separate dummy continuation is required to initialize the detection of these bifurcations. We have also generalized the test functions for the orbit- and inclination-flip bifurcations such that they can now be applied when the leading eigenvalues are complex. Note that in generic systems orbit- and inclination-flip bifurcations with complex eigenvalues have codimension 2.

MATCONT supports several straightforward methods to initialize homoclinic orbits, including one that is based on the approximation of the homoclinic orbit by a limit cycle with large period. However, there are many ODEs (e.g., describing traveling impulses) where the corresponding limit cycles are of the saddle type and cannot be found by numerical integration. Often such cycles are not born via local Hopf-like bifurcations. In such cases, the only known alternative for the initialization is a homotopy method by Doedel et al. [1994, 1997b]. In this article, we rigourously describe a generalization of the method and give implementation details for HHS orbits, but also for orbits homoclinic-to-saddle-node and heteroclinic orbits. To some extent, HomCont also supports the homotopy method. However, it is fully implemented only for orbits homoclinic-to-hyperbolic-saddle. We illustrate the effectiveness of the homotopy method by numerous examples (also in 4D with stable and unstable invariant 2D-manifolds), which should convince the reader of its robustness. Another aspect is that the first step in the homotopy method can be done either by a time integration or a continuation. In HomCont, the first step is done by continuation. We have tested both strategies, and in our examples the time-integration seemed to be the most effective. That is why in MATCONT the homotopy always starts from a solution obtained via the time integration.

We admit that the use of the homotopy method in MATCONT requires a certain degree of background knowledge of the method and the software. However, the user can execute the homotopy and standard continuation steps in a fairly easy way in the graphical interface (GUI) in MATCONT. The successive steps are logical to handle, which is not always the case in AUTO/HomCont, where dummy steps and "overspecified parameters" are routinely used, and where the homotopy method is recommended only for "expert users". Indeed, HomCont can only be run in AUTO Command Mode or using scripts. Preparing such commands and scripts, while studying connecting orbits in a concrete ODE system, requires creating several input files and browsing of several output files, which assumes a good understanding of their formats by the user. On the contrary, MATCONT users interact only with its GUI and never work directly with the low-level input and output files. Thus, the interactive initialization and continuation of homoclinic and heteroclinic orbits – organized via a specially designed GUI – is a major new feature of MATCONT that distinguishes it from any other software.

Some results of this article were briefly announced in Friedman et al. [2005].

2. EXTENDED DEFINING SYSTEM FOR CONTINUATION

2.1 Homoclinic-to-Hyperbolic-Saddle Orbits

Suppose that the eigenvalues of the Jacobian matrix $f_x(x_0, \alpha_0)$ can be ordered according to

$$\Re(\mu_{n_S}) \leq ... \leq \Re(\mu_1) < 0 < \Re(\lambda_1) \leq ... \leq \Re(\lambda_{n_U}),$$

where $\Re()$ stands for "real part of", n_S is the number of stable, and n_U the number of unstable eigenvalues.

2.1.1 Defining System. To continue HHS orbits in two free parameters, we use an extended defining system that consists of several parts.

First, the infinite time interval is truncated, so that instead of $[-\infty, +\infty]$ we use $[-T, +T]$, where T is the half-return time. This interval is rescaled to [0, 1] and divided into mesh intervals where the solution is approximated by a vector polynomial. N is the number of mesh intervals and m the degree of the piecewise polynomials. The mesh is nonuniform and adaptive. Each mesh interval is further subdivided by equidistant fine mesh points. Also, each mesh interval contains a number of collocation points. The equation

$$\dot{x}(t) - 2Tf(x(t), \alpha) = 0, \tag{2}$$

must be satisfied in each collocation point. (This discretization is the same as that for the limit cycles in AUTO [Doedel et al. 1997a] and CONTENT [Kuznetsov and Levitin 1998].)

The second part is the equilibrium condition

$$f(x_0, \alpha) = 0. \tag{3}$$

Third, there is a so-called phase condition for the homoclinic solution, that is not always used but helps to improve the continuation of the homoclinic solution:

$$\int_0^1 \dot{\widetilde{x}}^*(t)[x(t) - \widetilde{x}(t)]dt = 0. \tag{4}$$

Here $\widetilde{x}(t)$ is some initial guess for the solution, typically obtained from the previous continuation step. We note that in the literature another phase condition is also used (see, e.g., Doedel and Friedman [1989]). However, in the present implementation, we employ condition (4).

Fourth, there are the homoclinic-specific constraints to the solution. For these we need access to the stable and unstable eigenspaces of the system linearized about the equilibrium after each step. It is not efficient to recompute these spaces from scratch in each continuation-step. Instead, we use the algorithm for continuing invariant subspaces using only algebraic arguments, a modification of the method from Dieci and Friedman [2001], Demmel et al. [2000], and Bindel et al. [2008]. We now summarize the steps in this algorithm; details and an extensive algebraic justification are given in Ghaziani et al. [2009].

Suppose we have the following block Schur factorization for $A(0) = f_x(x_0, \alpha_0)$, the Jacobian matrix at the equilibrium point of a known homoclinic orbit, taken as a base point for the continuation:

$$A(0) = Q(0)\, R(0)\, Q^{\mathrm{T}}(0), \quad Q(0) = [Q_1(0)\, Q_2(0)],$$

where $A(0)$, $R(0)$ and $Q(0)$ are $n \times n$-matrices, $Q(0)$ is orthogonal, $Q_1(0)$ has dimensions $n \times m$ and $R(0)$ is block upper triangular

$$R(0) = \begin{bmatrix} R_{11} & R_{12} \\ 0 & R_{22} \end{bmatrix},$$

where R_{11} is an $m \times m$-block (R_{11} and R_{22} are not required to be triangular). Then the columns of $Q_1(0)$ span an invariant subspace $P(0)$ of dimension m (e.g., the stable or unstable subspace) of $A(0)$, and the columns of $Q_2(0)$ span the orthogonal complement $P(0)^{\perp}$.

What we need for the continuation are the subspace-defining columns for a matrix $A(s)$ close to $A(0)$, without having to compute everything explicitly again; we will call them $Q_1(s)$ and $Q_2(s)$:

$$A(s) = Q(s)\, R(s)\, Q^{\mathrm{T}}(s), \quad Q(s) = [Q_1(s)\, Q_2(s)],$$

where s parameterizes the curve of homoclinic orbits.

As shown in Dieci and Eirola [1999], it is always possible to obtain a smooth path of block Schur factorizations, and we can accumulate all transformations in such a way that we are always looking for corrections close to the identity. Thus, we can write (for s sufficiently small)

$$Q(s) = Q(0)\, U(s), \quad U(0) = I, \tag{5}$$

so that we now need to compute the $n \times n$-matrix $U(s)$. Partitioning $U(s)$ in blocks of the same size as we partitioned $R(0)$, we have

$$U(s) = [U_1(s)\, U_2(s)] = \begin{bmatrix} U_{11}(s) & U_{12}(s) \\ U_{21}(s) & U_{22}(s) \end{bmatrix},$$

where $U_{11}(s)$ has dimensions $m \times m$, and $U_{22}(s)$ dimensions $(n-m) \times (n-m)$.

In Ghaziani et al. [2009], it is proven that we can always assume that $U_{11}(s)$ and $U_{22}(s)$ are symmetric positive-definite, by redefining $Q(s)$ and $R(s)$ if necessary. Now define for all s the $(n-m) \times m$-matrix $Y(s)$ as

$$Y(s) = U_{21}(s) U_{11}^{-1}(s).$$

It is shown in Bindel et al. [2008] and Ghaziani et al. [2009] that $U(s)$ can be written completely in terms of $Y(s)$:

$$U(s) = \left[\begin{pmatrix} I \\ Y(s) \end{pmatrix} (I + Y(s)^{\mathrm{T}} Y(s))^{(-1/2)} \quad \begin{pmatrix} -Y(s)^{\mathrm{T}} \\ I \end{pmatrix} (I + Y(s) Y(s)^{\mathrm{T}})^{(-1/2)} \right]. \tag{6}$$

We now define $T_{11}(s)$, $T_{12}(s)$, $T_{21}(s)$ and $T_{22}(s)$ by

$$Q(0)^{\mathrm{T}}\, A(s)\, Q(0) = \begin{bmatrix} T_{11}(s) & T_{12}(s) \\ T_{21}(s) & T_{22}(s) \end{bmatrix}. \tag{7}$$

Here $T_{11}(s)$ is of size $m \times m$ and $T_{22}(s)$ is an $(n-m) \times (n-m)$-matrix. Using the invariant subspace relation

$$Q_2^{\mathrm{T}}(s)\, A(s)\, Q_1(s) = 0,$$

and executing substitutions using (5), (6), and (7), we obtain the following algebraic Riccati equation for $Y(s)$:

$$T_{22}(s)\, Y(s) - Y(s)\, T_{11}(s) + T_{21}(s) - Y(s)\, T_{12}(s)\, Y(s) = 0. \tag{8}$$

So to do a quick and smooth subspace continuation of both stable and unstable subspaces, we only need to keep track of two small matrices $Y_S(s) \in \mathbb{R}^{(n-n_S)\times n_S}$ (with S for stable) and $Y_U(s) \in \mathbb{R}^{(n-n_U)\times n_U}$ (with U for unstable). We use a similar notation for the stable and unstable variants of $T_{11}(s)$, $T_{12}(s)$, $T_{21}(s)$ and $T_{22}(s)$. From the matrices $Y_S(s)$ and $Y_U(s)$, we can easily compute the span of the stable and unstable subspaces, and their orthogonal complements.

Equation (8) is added to the dynamical system to keep track of matrices $Y_S(s)$ and $Y_U(s)$, which are obtained from the separate Riccati equations

$$\begin{aligned} T_{22U}(s)Y_U(s) - Y_U(s)T_{11U}(s) + T_{21U}(s) - Y_U(s)T_{12U}(s)Y_U(s) &= 0, \\ T_{22S}(s)\,Y_S(s) - Y_S(s)\,T_{11S}(s) + T_{21S}(s) - Y_S(s)\,T_{12S}(s)\,Y_S(s) &= 0. \end{aligned} \tag{9}$$

Now we can formulate constraints on the behavior of the solution close to the equilibrium x_0. The initial vector of the orbit, $(x(0) - x_0)$, is placed in the unstable eigenspace of the system in the equilibrium. We express this by the requirement that it is orthogonal to the orthogonal complement of the unstable eigenspace. Analogously, the end vector of the orbit, $(x(1) - x_0)$, is placed in the stable eigenspace of the system in the equilibrium. This is expressed by the requirement that the vector is orthogonal to the orthogonal complement of the stable eigenspace.

From (5) and (6), if $Q_U(0)$ is the orthogonal matrix from the base point related to the unstable invariant subspace, then a basis of that subspace in another point can be computed by

$$Q^U(s) = Q_U(0)\begin{bmatrix} I \\ Y_U(s) \end{bmatrix},$$

while a basis for the orthogonal complement to that subspace can be computed by

$$Q^{U^\perp}(s) = Q_U(0)\begin{bmatrix} -Y_U(s)^{\mathrm{T}} \\ I \end{bmatrix}.$$

Note that in general the bases $Q^U(s)$ and $Q^{U^\perp}(s)$ are not orthogonal. The matrices for the stable subspace can be computed similarly. The equations to be added to the system are

$$\begin{aligned} Q^{U^\perp}(s)^{\mathrm{T}}(x(0) - x_0) &= 0, \\ Q^{S^\perp}(s)^{\mathrm{T}}(x(1) - x_0) &= 0. \end{aligned} \tag{10}$$

The initial values of $Y_U(0)$, $Y_S(0)$ in the base point are zero matrices.

Finally, the distances between $x(0)$ (resp. $x(1)$) and x_0 must be taken into account, so that

$$\begin{aligned} \left\| x(0) - x_0 \right\| - \epsilon_0 &= 0, \\ \left\| x(1) - x_0 \right\| - \epsilon_1 &= 0. \end{aligned} \tag{11}$$

These distances ϵ_0 and ϵ_1 should be small enough. The half-return time T, ϵ_0 and ϵ_1 are called the homoclinic parameters.

After a user-chosen number of steps, the base point is adapted. This means that $Q_U(0)$ and $Q_S(0)$ are recomputed, Y_U and Y_S are reset to zero, and the mesh is adapted.

2.1.2 Implementation in MATCONT. The basic defining system for the continuation of a HHS orbit in two free system parameters consists of (2), (3), (9), (10), and (11) with T free and ϵ_0 and ϵ_1 fixed, so that the phase condition (4) is not used.

Alternatively, the phase condition (4) is added automatically if from the triple (T, ϵ_0, ϵ_1) two homoclinic parameters are freed, instead of just one. Any combination of one or two parameters of that triple is possible.

The variables in the defining system are stored in one vector. It contains the values of $x(t)$ in the fine mesh points (including $x(0)$ and $x(1)$), the free homoclinic parameters, two free system parameters, the coordinates of the saddle x_0, and the elements of the matrices Y_S and Y_U.

2.2 Homoclinic-to-Saddle-Node Orbits

When x_0 is a saddle-node, the eigenvalues of $f_x(x_0, \alpha_0)$ can be ordered as

$$\Re(\mu_{n_S}) \leq \ldots \leq \Re(\mu_1) < \nu_1 = 0 < \Re(\lambda_1) \leq \ldots \leq \Re(\lambda_{n_U}),$$

where n_S is the number of stable, and n_U the number of unstable eigenvalues.

For a homoclinic orbit to a saddle-node equilibrium, the extended defining system undergoes some small changes. Now the vector $(x(0) - x_0)$ has to be placed in the center-unstable subspace, instead of the unstable space. Analogously, $(x(1) - x_0)$ must be in the center-stable subspace. Thus, one of these spaces has one extra eigenvector and one less restriction.

The vector-condition again is implemented by requiring that the vector is orthogonal to the orthogonal complement of the corresponding space. So the equations (10) themselves do not really change; the changes happen in the computation of the matrices Q. One of these matrices now has one less column, so there is one condition less.

The number of equations is restored however, by adding the constraint that the equilibrium must be a saddle-node, i.e. has eigenvalue $\nu = 0$. For this we use the bordering technique, as described in Section 4.2.1 of Govaerts [2000]. The technique basically requires g to be zero, where g is obtained by solving

$$\begin{pmatrix} f_x(x_0, \alpha) & w_{bor} \\ v_{bor}^{\mathrm{T}} & 0 \end{pmatrix} \begin{pmatrix} v \\ g \end{pmatrix} = \begin{pmatrix} 0 \\ 1 \end{pmatrix}. \tag{12}$$

Here w_{bor} and v_{bor} are bordering vectors, chosen in such a way that the matrix in (12) is nonsingular. These vectors have to be adapted at the adaptation points.

Taking the previous remarks into account, the defining system for the continuation of HSN orbits is given by (2) – (3) – ($g = 0$) – (4) – (9) – (10) – (11).

3. STARTING STRATEGIES

In this section we examine two ways in which the continuation of HHS orbits in MATCONT can be initialized: either from a limit cycle with large period, or using the homotopy method, starting from a saddle equilibrium. Starting from a Bogdanov-Takens equilibrium point is also implemented but will not be dealt with in this article, details can be found in Beyn et al. [2002].

3.1 Starting from a Limit Cycle with Large Period

When starting from a limit cycle with large period, the user must first declare the cycle to be close to a homoclinic-to-hyperbolic-saddle orbit. Automatically, initial values for the homoclinic parameters will be computed, as in HomCont. First, the program looks for the point on the cycle with smallest $\| f(x, \alpha) \|$. This point is taken as a first approximation for the equilibrium x_0.

The mesh points of the limit cycle are kept as mesh points for the homoclinic orbit, except for the mesh interval that contains the current equilibrium approximation. This mesh interval is deleted, as it will grow to infinity in the homoclinic orbit. In

memory, the stored cycle then needs to be 'rotated', so that the first and last point of the homoclinic orbit ($x(0)$ and $x(1)$) are effectively stored as first and last point, respectively. Half of the period of the remaining part of the cycle is kept as initial value for T. Initial values for ϵ_0 and ϵ_1 are also computed; these are found by simply computing the distance from $x(0)$ and $x(1)$ to the approximated equilibrium.

Then, the user has to select 2 free system parameters, and 1 or 2 of the homoclinic parameters T, ϵ_0, ϵ_1. The defining system (i.e., the number of equations) is automatically adjusted according to the choice of the user.

3.2 Starting by Homotopy

3.2.1 The Method. For the initialization of HHS orbits, there is an efficient method that constructs a homoclinic-to-hyperbolic-saddle orbit starting from only the saddle equilibrium $x_0^{(0)}$.

As described in Section 2.1, the defining equations for the continuation of a homoclinic orbit can be written as

$$\begin{aligned}
&\dot{x}(t) - 2Tf(x(t), \alpha) = 0,\\
&f(x_0, \alpha) = 0,\\
&\textstyle\int_0^1 \tilde{\dot{x}}^*(t)[x(t) - \tilde{x}(t)]dt = 0,\\
&Q^{U^\perp,\mathrm{T}}(x(0) - x_0) = 0,\\
&Q^{S^\perp,\mathrm{T}}(x(1) - x_0) = 0,\\
&T_{22U}Y_U - Y_U T_{11U} + T_{21U} - Y_U T_{12U} Y_U = 0,\\
&T_{22S}Y_S - Y_S T_{11S} + T_{21S} - Y_S T_{12S} Y_S = 0,\\
&\left\|x(0) - x_0\right\| - \epsilon_0 = 0,\\
&\left\|x(1) - x_0\right\| - \epsilon_1 = 0,
\end{aligned} \tag{13}$$

where $Q^{U^\perp} \in \mathbb{R}^{n\times n_S}$, $Q^{S^\perp} \in \mathbb{R}^{n\times n_U}$, $Y_U \in \mathbb{R}^{n_S\times n_U}$ and $Y_S \in \mathbb{R}^{n_U\times n_S}$.

If the phase condition is added, two of the three homoclinic parameters $T, \epsilon_0, \epsilon_1$ are needed, otherwise only one homoclinic parameter is needed. Without phase condition the number of constraints is equal to $Nmn + 2n + 2 + 2n_U n_S$. The free scalar variables are given by $x_M, x_0, \alpha_1, T, Y_U, Y_S$, where x_M denotes the vector of the function values at the fine mesh points and α_1 is the free system parameter, so that the number of free scalar variables equals $Nmn + 2n + 2 + 2n_U n_S$. If the phase condition is added, the number of constraints is augmented by one and an extra homoclinic parameter has to be freed. For continuation a second parameter has to be freed.

Initially the projections $Q^{U^\perp,(0)}$ and $Q^{S^\perp,(0)}$ are constructed using the real Schur factorizations:

$$\begin{aligned}
f_x(x_0^{(0)}, \alpha) &= Q_0^{(0)} R_0^{(0)} Q_0^{(0),T}, \quad & Q_0^{(0)} &= [Q^{U,(0)}\ Q^{U^\perp,(0)}],\\
f_x(x_0^{(0)}, \alpha) &= Q_1^{(0)} R_1^{(0)} Q_1^{(0),T}, \quad & Q_1^{(0)} &= [Q^{S,(0)}\ Q^{S^\perp,(0)}].
\end{aligned} \tag{14}$$

These first factorizations are chosen so that the n_U columns $q_{0,1}^{(0)}, ..., q_{0,n_U}^{(0)}$ of $Q^{U,(0)}$ form an orthonormal basis of the right invariant subspace S_0^U of $f_x(x_0^{(0)}, \alpha)$, corresponding to the eigenvalues $\lambda_1^{(0)}, ..., \lambda_{n_U}^{(0)}$, and the $n_S = n - n_U$ columns $q_{0,n_U+1}^{(0)}, ..., q_{0,n_U+n_S}^{(0)}$ of $Q^{U^\perp,(0)}$ form an orthonormal basis of the orthogonal complement $S_0^{U^\perp}$. Similarly, the n_S columns $q_{1,1}^{(0)}, ..., q_{1,ns}^{(0)}$ of $Q^{S,(0)}$ form an orthonormal basis of the right invariant subspace S_0^S of $f_x(x_0^{(0)}, \alpha)$, corresponding to the eigenvalues $\mu_1^{(0)}, ..., \mu_{n_S}^{(0)}$, and the n_U

columns $q^{(0)}_{1,n_S+1}, ..., q^{(0)}_{1,n_S+n_U}$ of $Q^{S^\perp,(0)}$ form an orthonormal basis of the orthogonal complement $S_0^{S^\perp}$.

Moreover, let $S^U_{0,k}$, $k = 1, ..., n_U$, be the right invariant subspace of $f_x(x_0^{(0)}, \alpha)$ corresponding to the eigenvalues $\lambda_1^{(0)}, ..., \lambda_k^{(0)}$, whenever either $\lambda_k^{(0)}$ is real or $(\lambda_{k-1}^{(0)}, \lambda_k^{(0)})$ form a conjugate pair of complex eigenvalues. Then the first k columns $q^{(0)}_{0,1}, ..., q^{(0)}_{0,k}$ of $Q_0^{(0)}$ form an orthonormal basis of $S^U_{0,k}$ and the remaining $n-k$ columns $q^{(0)}_{0,k+1}, ..., q^{(0)}_{0,n}$ of $Q_0^{(0)}$ form an orthonormal basis of the orthogonal complement $S^{U^\perp}_{0,k}$. The analog holds for the subspace corresponding to the negative eigenvalues.

The construction process of a homoclinic orbit fitting the above equations (13), from a saddle equilibrium, is splitted into several steps in the algorithm in 3.2.2. The basic ideas of this homotopy method were formulated in Doedel et al. [1994, 1997b]. We first give the outline of the algorithm and in Section 3.2.2 we write down the explicit equations.

The beginning vector $x(0) - x_0$ of a homoclinic orbit lies in the eigenspace of the leading unstable eigenvalues, that is, λ_1 if this eigenvalue is real, or λ_1 and λ_2 if they form a conjugate complex pair. We start by choosing an initial point in this space, not far from the saddle equilibrium $x_0^{(0)}$, say $x(0) = x_0^{(0)} + \epsilon_0(c_1 q^{(0)}_{0,1} + c_2 q^{(0)}_{0,2})$. Here, c_2 is nonzero only when λ_1 and λ_2 form a conjugate pair. Now there are two possibilities. Either, we obtain an initial connecting orbit by time integration, starting from the above-mentioned point $x(0)$. Or, we initialize a small connecting orbit segment $[0, T]$ by the constant $x(0)$ and extend this initial orbit segment by continuation with respect to T.

Define $\tau_i = \frac{1}{\epsilon_1}\langle x(1) - x_0^{(0)}, q^{(0)}_{1,n_S+i}\rangle$, for $i = 1, \ldots n_U$. Typically, the initial connecting orbit is a crude orbit with initial point $x(0) \in S_0^U$ but the terminal point $x(1) \notin S_0^S$. Hence, the τ_i's are, in general, nonzero. For an HHS orbit holds that $x(1) \in S_0^S$ so $\tau_i = 0$, for $i = 1, \ldots n_U$. By a sequence of homotopies, we will locate zero intercepts of the τ_i's.

Define now c_i as $c_i = \frac{1}{\epsilon_0}\langle x(0) - x_0^{(0)}, q^{(0)}_{0,i}\rangle$, for $i = 1, \ldots, n_U$. This is consistent with the use of c_1 and c_2 in the previous definition of $x(0)$. In the first homotopy, we try to locate a zero intercept of one of the τ_i's. All τ_i's are free and both c_1 and c_2 are free under the restriction that $c_1^2 + c_2^2 = 1$, since $\|x(0) - x_0\| = \epsilon_0$. In the following homotopy steps, we fix all τ_j's that are zero already, and try to locate a zero of another τ_i, while each time freeing an additional c_i, to replace the fixed equation $\tau_j = 0$ and thus to keep the same number of free variables. So, in the successive steps we let the initial point $x(0)$ vary within a wider subspace of the unstable eigenspace S_0^U of $x_0^{(0)}$ in order to place the end point $x(1)$ in the stable eigenspace S_0^S of $x_0^{(0)}$. More specifically, we keep $x(1)$ free, while $x(0)$ is allowed to vary on the hypersphere in S_0^U of radius ϵ_0.

In the previous successive homotopies, zero intercepts are detected of all τ_i except for one. This last τ_i can be made zero, by varying one component of the system parameter α. This requires recalculation of the saddle equilibrium x_0, and of the matrices $Q^{U^\perp}$ and $Q^{S^\perp}$, by use of the matrices Y_U and Y_S. When having detected a zero intercept of the last τ_i, the end vector $x(1) - x_0$ lies within the stable eigenspace S_0^S of x_0. However, the distance ϵ_1 is not necessarily small. Therefore, one more continuation, with T, ϵ_1 and one system parameter free, is needed to make ϵ_1 small enough in order to find a proper starting orbit for the continuation of homoclinic orbits.

In each homotopy step, we compute a branch, that is, a one-dimensional manifold, of solutions. For this, we must have $n_c - n_v = -1$, where n_c is the number of constraints, and n_v is the number of free scalar variables.

The described procedure converges, provided the initialization is sufficiently close to the homoclinic situation, see convergence theorem in Doedel et al. [1997b].

3.2.2 The Algorithm. We recall that in MATCONT the discretization is done by orthogonal collocation using piecewise polynomials. Let x_M be the vector of the function values at the fine mesh points. We denote x_C as the vector of the function values at the collocation points, more specifically at the Gauss points, and $\dot{x}_C$ as the vector of the derivative values at the Gauss points.

Having clarified the notation, we can now describe the algorithm in detail.

ALGORITHM 1. Locating a homoclinic orbit by homotopy.

Input.

$x_0^{(0)} \in \mathbb{R}^n$, $\alpha \in \mathbb{R}^p$, $f_x(x_0^{(0)}, \alpha)$, and the real Schur factorizations (14).

(1) **Locating a connecting orbit, α is fixed.**

Step 1. We have already noted that either a time integration or a continuation can be used to compute an initial connecting orbit. With time integration, the starting point is

$$x(0) = x_0^{(0)} + \epsilon_0(c_1 q_{0,1}^{(0)} + c_2 q_{0,2}^{(0)}),$$

where c_2 is zero, except in the case that the eigenvalues with smallest positive real part consist of a conjugate complex pair. Note that $c_1^2 + c_2^2 = 1$ and $c_3 = \cdots = c_{n_U} = 0$.

If continuation is used, set the algorithm parameters ϵ_0 and T to small, positive values, so that $x(t)$ is approximately constant on $[0, T]$, or after rescaling on $[0, 1]$. To be specific, set

$$x(t) = x_0^{(0)} + \epsilon_0(c_1 q_{0,1}^{(0)} + c_2 q_{0,2}^{(0)}), \quad 0 \le t \le 1,$$

with the same remark for c_2 as above. Extend this small starting segment by continuation where the equations are given by

$$\begin{aligned}
&\dot{x}_C - 2Tf(x_C, \alpha) = 0,\\
&\epsilon_0 c_i - \langle x(0) - x_0^{(0)}, q_{0,i}^{(0)}\rangle = 0, \quad i = 1, ..., n_U,\\
&\tau_i - \tfrac{1}{\epsilon_1}\langle x(1) - x_0^{(0)}, q_{1,n_S+i}^{(0)}\rangle = 0, \quad i = 1, ..., n_U,\\
&\langle x(0) - x_0^{(0)}, q_{0,n_U+i}^{(0)}\rangle = 0, \quad i = 1, ..., n_S,\\
&\|x(1) - x_0^{(0)}\| - \epsilon_1 = 0.
\end{aligned} \tag{15}$$

This gives us $n_c = Nmn + n + n_U + 1$ constraints and the free scalar variables are $x_M, \tau_1, \ldots, \tau_{n_U}, T, \epsilon_1$ so that $n_v = Nmn + n + n_U + 2$. Therefore, it is possible to compute a branch of solutions to system (15) in the direction of increasing T.

Typically ϵ_1 initially increases and then starts to decrease. In practice, one usually executes time-integration or continuation until ϵ_1 stops decreasing, its value being not necessarily small.

Steps k, k = 2, ..., n_U (for $n_U > 1$). Compute a branch of solutions to the system

$$\begin{aligned}
&\dot{x}_C - 2Tf(x_C, \alpha) = 0,\\
&\epsilon_0 c_i - \langle x(0) - x_0^{(0)}, q_{0,i}^{(0)}\rangle = 0, \quad i = 1, ..., n_U,\\
&\tau_i - \tfrac{1}{\epsilon_1}\langle x(1) - x_0^{(0)}, q_{1,n_S+i}^{(0)}\rangle = 0, \quad i = 1, ..., n_U,\\
&\langle x(0) - x_0^{(0)}, q_{0,n_U+i}^{(0)}\rangle = 0, \quad i = 1, ..., n_S,\\
&\|x(0) - x_0^{(0)}\| - \epsilon_0 = 0,\\
&\|x(1) - x_0^{(0)}\| - \epsilon_1 = 0,
\end{aligned}$$

to locate a zero of, say, τ_{k-1} (while $\tau_1, ..., \tau_{k-2} = 0$ are fixed). Free scalar variables are $x_M, c_1, ..., c_k, \tau_{k-1}, ..., \tau_{n_U}, \epsilon_1$. Therefore, there are $n_c = Nmn + n + n_U + 2$ constraints and $n_v = Nmn + n + n_U + 3$ free scalar variables, so $n_c - n_v = -1$.
At the end of these successive steps, all the τ's are zero except for one. Remark that zero intercepts of the τ_i's don't have to be located in the order $\tau_1, \tau_2, \ldots$, any order is possible.

(2) **Locating a connecting orbit, α varies.**
Step $n_U + 1$. Compute a branch of solutions to the system

$$\begin{aligned}
&\dot{x}_C - 2Tf(x_C, \alpha) = 0,\\
&f(x_0, \alpha) = 0,\\
&\langle x(0) - x_0, q_{0,n_U+i}\rangle = 0, \quad i = 1, ..., n_S,\\
&\tau_i - \tfrac{1}{\epsilon_1}\langle x(1) - x_0, q_{1,n_S+i}\rangle = 0, \quad i = 1, ..., n_U,\\
&T_{22U}Y_U - Y_U T_{11U} + T_{21U} - Y_U T_{12U} Y_U = 0,\\
&T_{22S}Y_S - Y_S T_{11S} + T_{21S} - Y_S T_{12S} Y_S = 0,\\
&\left\|x(0) - x_0\right\| - \epsilon_0 = 0,\\
&\left\|x(1) - x_0\right\| - \epsilon_1 = 0,
\end{aligned}$$

where $Y_U \in \mathbb{R}^{n_S \times n_U}, Y_S \in \mathbb{R}^{n_U \times n_S}$, to locate a zero of τ_{n_U} (while $\tau_1, ..., \tau_{n_U-1} = 0$ are fixed). Free scalar variables are $x_M, x_0, \alpha_1, \tau_{n_U}, \epsilon_1, Y_U, Y_S$. This gives us $n_c = Nmn + 2n + 2 + 2n_U n_S$ constraints and $n_v = Nmn + 2n + 3 + 2n_U n_S$ free scalar variables, so $n_c - n_v = -1$.
Now, the end vector $x(1) - x_0$ lies within the stable eigenspace of the saddle equilibrium.

(3) **Increasing the accuracy of the connecting orbit, α varies**.
Step $n_U + 2$. Compute a branch of solutions to the system

$$\begin{aligned}
&\dot{x}_C - 2Tf(x_C, \alpha) = 0,\\
&f(x_0, \alpha) = 0,\\
&\langle x(0) - x_0, q_{0,n_U+i}\rangle = 0, \quad i = 1, ..., n_S,\\
&\langle x(1) - x_0, q_{1,n_S+i}\rangle = 0, \quad i = 1, ..., n_U,\\
&T_{22U}Y_U - Y_U T_{11U} + T_{21U} - Y_U T_{12U} Y_U = 0,\\
&T_{22S}Y_S - Y_S T_{11S} + T_{21S} - Y_S T_{12S} Y_S = 0,\\
&\left\|x(0) - x_0\right\| - \epsilon_0 = 0,\\
&\left\|x(1) - x_0\right\| - \epsilon_1 = 0,
\end{aligned}$$

where $Y_U \in \mathbb{R}^{n_S \times n_U}, Y_S \in \mathbb{R}^{n_U \times n_S}$, in the direction of decreasing ϵ_1 until this distance is 'small'. Free scalar variables are $x_M, x_0, \alpha_1, T, \epsilon_1, Y_U, Y_S$. As before, $n_c = Nmn + 2n + 2 + 2n_U n_S$ and $n_v = Nmn + 2n + 3 + 2n_U n_S$.

By executing the successive steps of the algorithm, a connecting orbit is constructed with the beginning vector lying in the unstable eigenspace of the saddle equilibrium, the end vector lying in the stable eigenspace and ϵ_0 and ϵ_1 small. Now, the continuation of HHS orbits can be started, making use of system (13).

3.2.3 Implementation in MATCONT. In MATCONT, the initial connecting orbit in the first step is obtained by time-integration since in our experiments this approach led to more stable results. Further, the c_i's are denoted as UParam1, UParam2, etc. (the notation refers to unstable connection parameters) and the τ_i's are denoted as SParam1, SParam2, etc. (the notation refers to stable connection parameters). In the Type menu

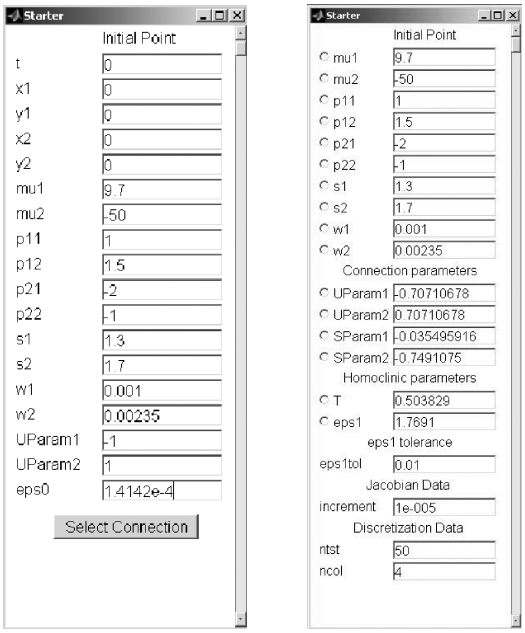

Fig. 1. Starter windows.

in the MatCont window, the curve type of the initial orbit is ConnectionSaddle and the curve type of the successive continuations is denoted as HomotopySaddle. In the MatCont window, these curve types are abbreviated to ConnecHom and HTHom. So the curve of the time-integration appears in the MatCont window as `EP_ConnecHom` and the possible continuations as `ConnecHom_HTHom, HTHom_HTHom, HTHom_Hom`.

We now consider the Starter windows of the successive curves. The left Starter of Figure 1 shows the Starter window of `EP_ConnecHom`. The coordinates of the saddle equilibrium $x_0^{(0)}$, the system parameters, UParam1 and UParam2 and the distance ϵ_0 have to be filled in by the user. When the eigenvalue with smallest positive real part is real, only UParam1 is taken into account (whatever value to UParam2 is given). Then two opposite directions are candidates for the position of the starting point $x(0)$, dependent on the sign of UParam1. When the eigenvalues with smallest positive real part consist of a conjugate complex pair, the starting point is determined by $x(0) = x_0^{(0)} + \epsilon_0(\text{UParam1}\, q_{0,1}^{(0)} + \text{UParam2}\, q_{0,2}^{(0)})$. So the beginning vector can lie in a two-dimensional space, which doesn't make it obvious at all in which direction we have to start. Only trial and error helps in this case.

To make it easier for the user when choosing the unstable connection parameters, the condition $\text{UParam1}^2 + \text{UParam2}^2 = 1$ can be ignored in the first step. UParam1 and UParam2 are automatically rescaled by MATCONT so that this condition is fulfilled.

When the user obtains a satisfactory connecting orbit after time integration, the button "Select Connection" has to be pressed. The user can then choose the number of mesh intervals and collocation points. By standard, 40 mesh intervals and 4 collocation points are used. The code now searches for the point on the time-integrated orbit where ϵ_1 stops decreasing for the last time. If such a point doesn't exist, the last point of the orbit is taken. This point is selected as the end point of the initial connecting orbit.

The starter window for `ConnecHom_HTHom` and `HTHom_HTHom` is illustrated on the right side of Figure 1. In the successive continuations, the user has to indicate the free system parameter, the free connection parameters and the free homoclinic parameters. Error catches are provided. If, for example, a stable connection parameter equal to zero is denoted as free, an error window appears.

In the successive continuations, which locate zero intercepts of the SParams, a test function determines whether a SParam has become zero. This test function is the product of the free stable connection parameters. In the continuation to make ϵ_1 small, the test function is given by ϵ_1−eps1tol, where eps1tol is a tolerance, choosen by the user, which determines how small ϵ_1 is wanted.

We give examples of the method in 6.1 and 6.2.

4. STARTING BY HOMOTOPY: HSN ORBITS AND HETEROCLINIC ORBITS

We have also implemented variants of the homotopy method for HSN orbits and heteroclinic orbits.

4.1 Starting by Homotopy: Homoclinic to Saddle-Node Orbits

4.1.1 The Method. In the homotopy method for HSN orbits, we start from a saddle-node equilibrium $x_0^{(0)}$ to construct a homoclinic to saddle-node orbit. The defining equations for the continuation of a HSN orbit consist of (13), where $Q^{U^\perp} \in \mathbb{R}^{n\times n_S}$, $Q^{S^\perp} \in \mathbb{R}^{n\times n_U}$ as before, but $Y_U \in \mathbb{R}^{(n_S+1)\times n_U}$ and $Y_S \in \mathbb{R}^{(n_U+1)\times n_S}$, supplemented by the equation

$$g = 0, \tag{16}$$

where g is computed by solving (12). If the phase condition is added, two of the three homoclinic parameters $T, \epsilon_0, \epsilon_1$ are needed, otherwise only one homoclinic parameter is needed. Without phase condition, the number of constraints equals $Nmn + 2n + 2 + (n_S + 1)n_U + (n_U + 1)n_S$ and $x_M, x_0, \alpha_1, T, Y_U, Y_S$ are the free scalar variables so $n_v = Nmn + 2n + 2 + (n_S+1)n_U + (n_U+1)n_S$. If the phase condition is added, the number of constraints is augmented by one and an extra homoclinic parameter has to be freed. For continuation, a second parameter has to be varied so that $n_c - n_v = -1$.

In (13)–(16), the columns of $Q^{U^\perp}$ span the orthogonal complement of the center-unstable eigenspace of the saddle-node equilibrium while the columns of $Q^{S^\perp}$ span the orthogonal complement of the center-stable eigenspace. As in the homotopy method for HHS orbits, initially these projections are constructed using the real Schur factorizations:

$$\begin{array}{ll} f_x(x_0^{(0)}, \alpha) = Q_0^{(0)} R_0^{(0)} Q_0^{(0),\mathrm{T}}, & Q_0^{(0)} = [Q^{U,(0)}\ Q^{U^\perp,(0)}], \\ f_x(x_0^{(0)}, \alpha) = Q_1^{(0)} R_1^{(0)} Q_1^{(0),\mathrm{T}}, & Q_1^{(0)} = [Q^{S,(0)}\ Q^{S^\perp,(0)}]. \end{array} \tag{17}$$

These first factorizations are choosen so that the $n_U + 1$ columns $q_{0,1}^{(0)}, ..., q_{0,n_U+1}^{(0)}$ of $Q^{U,(0)}$ form an orthonormal basis of the right invariant subspace S_0^U of $f_x(x_0^{(0)}, \alpha)$, corresponding to the eigenvalues $\lambda_1^{(0)}, ..., \lambda_{n_U}^{(0)}, \lambda_{n_U+1}^{(0)}$ (with $\lambda_{n_U+1}^{(0)} = \nu_1^{(0)}$) and the $n_S = n - n_U - 1$ columns $q_{0,n_U+1+i}^{(0)}$, $i = 1, \ldots, n_S$, of $Q^{U^\perp,(0)}$ form an orthonormal basis of the orthogonal complement $S_0^{U^\perp}$. Similarly, the $n_S + 1$ columns $q_{1,1}^{(0)}, ..., q_{1,n_S+1}^{(0)}$ of $Q^{S,(0)}$ form an orthonormal basis of the right invariant subspace S_0^S of $f_x(x_0^{(0)}, \alpha)$, corresponding to

the eigenvalues $\mu_1^{(0)}, ..., \mu_{nS}^{(0)}, \mu_{nS+1}^{(0)}$ (with $\mu_{nS+1}^{(0)} = \nu_1^{(0)}$), and the n_U columns $q_{1,nS+1+i}^{(0)}$, $i = 1, \ldots, n_U$, of $Q^{S^\perp,(0)}$ form an orthonormal basis of the orthogonal complement $S_0^{S^\perp}$.

Moreover, let $S_{0,k}^U$, $k = 1, ..., n_U + 1$, be the right invariant subspace of $f_x(x_0^{(0)}, \alpha)$ corresponding to the eigenvalues $\lambda_1^{(0)}, ..., \lambda_k^{(0)}$, whenever either $\lambda_k^{(0)}$ is real or $(\lambda_{k-1}^{(0)}, \lambda_k^{(0)})$ form a conjugate pair of complex eigenvalues. Then the first k columns $q_{0,1}^{(0)}, \ldots, q_{0,k}^{(0)}$ of $Q_0^{(0)}$ form an orthonormal basis of $S_{0,k}^U$ and the remaining $n-k$ columns $q_{0,k+1}^{(0)}, ..., q_{0,n}^{(0)}$ of $Q_0^{(0)}$ form an orthonormal basis of the orthogonal complement $S_{0,k}^{U^\perp}$. The analog holds for the subspace corresponding to the negative eigenvalues.

The construction process of a HSN orbit fitting equations (13)-(16) from a saddle-node equilibrium is analogous to the homotopy method for HHS orbits, although there are some essential differences. Let's first pay attention to this, before giving the explicit equations in 4.1.2.

The beginning vector of a HSN orbit lies in the eigenspace corresponding to the zero eigenvalue ν_1. Therefore, only two opposite directions are candidates for starting direction which makes it easier to find a proper initial connecting orbit.

Now, possibly n_U or n_S is equal to zero. If n_U equals zero, the center-stable space is the whole phase space so only one continuation in which ϵ_1 is made small needs to be executed.

Since the number of c's is one more than the number of τ's, no system parameter has to be varied in the series of continuations which makes the stable connection parameters zero. Indeed, when n_U is strictly positive, in the first homotopy step, two c's are free and all the τ's are free and, in the following steps, we let each time one more c free to replace the fixed equation $\tau = 0$. Also the continuation that makes ϵ_1 small requires no free system parameter.

4.1.2 The Algorithm. We now consider the algorithm in more detail.

ALGORITHM 2. Locating a homoclinic to saddle-node orbit by homotopy.

Input.

$x_0^{(0)} \in \mathbb{R}^n$, $f_x(x_0^{(0)}, \alpha)$, and the real Schur factorizations (17).

(1) **Locating a connecting orbit.**
Step 1. A HSN orbit starts in the direction of the eigenvector q corresponding to the zero eigenvalue ν_1. The first step of the homotopy method can be done either by time integration or continuation. If we choose time integration, we start from the point $x(0) = x_0^{(0)} + \epsilon_0 c_1 q^{(0)}$. The value of c_1 is either 1 or -1 and $c_2, \ldots, c_{n_U+1}$ are put equal to zero. If continuation is used, we set a small orbit segment equal to a constant, namely $x(t) = x_0^{(0)} + \epsilon_0 c_1 q^{(0)}$ in $[0, T]$ for small values of T and ϵ_0 and the same remark for the c's holds. We then extend this segment by continuation using the following equations:

$$
\begin{aligned}
&\dot{x}_C - 2Tf(x_C, \alpha) = 0,\\
&\epsilon_0 c_i - \langle x(0) - x_0^{(0)}, q_{0,i}^{(0)} \rangle = 0, \quad i = 1, ..., n_U + 1,\\
&\tau_i - \tfrac{1}{\epsilon_1} \langle x(1) - x_0^{(0)}, q_{1,n_S+1+i}^{(0)} \rangle = 0, \quad i = 1, ..., n_U,\\
&\langle x(0) - x_0^{(0)}, q_{0,n_U+1+i}^{(0)} \rangle = 0, \quad i = 1, ..., n_S,\\
&\|x(1) - x_0^{(0)}\| - \epsilon_1 = 0.
\end{aligned}
$$

This gives us $n_c = Nmn + n + n_U + 1$ constraints and the free scalar variables are $x_M, \tau_1, \ldots, \tau_{n_U}, T, \epsilon_1$ so $n_v = Nmn + n + n_U + 2$.

Again, typically ϵ_1 first increases and then starts to decrease. We stop the time integration or continuation when ϵ_1 stops decreasing.

Steps k, $k = 2, ..., n_U + 1$ ($n_U \geq 1$). Compute a branch of solutions to the system

$$\begin{aligned}
&\dot{x}_C - 2Tf(x_C, \alpha) = 0,\\
&\epsilon_0 c_i - \langle x(0) - x_0^{(0)}, q_{0,i}^{(0)} \rangle = 0, \quad i = 1, ..., n_U + 1,\\
&\tau_i - \tfrac{1}{\epsilon_1} \langle x(1) - x_0^{(0)}, q_{1,n_S+1+i}^{(0)} \rangle = 0, \quad i = 1, ..., n_U,\\
&\langle x(0) - x_0^{(0)}, q_{0,n_U+1+i}^{(0)} \rangle = 0, \quad i = 1, ..., n_S,\\
&\|x(0) - x_0^{(0)}\| - \epsilon_0 = 0,\\
&\|x(1) - x_0^{(0)}\| - \epsilon_1 = 0,
\end{aligned}$$

to locate a zero of, say, τ_{k-1} (while $\tau_1, \ldots, \tau_{k-2} = 0$ are fixed). The number of constraints is $n_c = Nmn + n + n_U + 2$ and the free scalar variables are given by $x_M, c_1, \ldots, c_k, \tau_{k-1}, \ldots, \tau_{n_U}, \epsilon_1$ so that $n_v = Nmn + n + n_U + 3$, and thus $n_c - n_v = -1$.

The τ's can be made zero in any possible order. At the end of these successive continuations the end vector $x(1) - x_0^{(0)}$ lies within the center-stable eigenspace of $x_0^{(0)}$.

(2) **Increasing the accuracy of the connecting orbit.**

Step $n_U + 2$. Compute a branch of solutions to the system

$$\begin{aligned}
&\dot{x}_C - 2Tf(x_C, \alpha) = 0,\\
&\langle x(0) - x_0^{(0)}, q_{0,n_U+1+i}^{(0)} \rangle = 0, \quad i = 1, ..., n_S,\\
&\langle x(1) - x_0^{(0)}, q_{1,n_S+1+i}^{(0)} \rangle = 0, \quad i = 1, ..., n_U,\\
&\|x(0) - x_0^{(0)}\| - \epsilon_0 = 0,\\
&\|x(1) - x_0^{(0)}\| - \epsilon_1 = 0,
\end{aligned}$$

in the direction of decreasing ϵ_1 until this distance is 'small'. The number of constraints is $n_c = Nmn + n + 1$ and the free scalar variables are x_M, T, ϵ_1 so that $n_v = Nmn + n + 2$.

The successive homotopies give a connecting orbit where the starting vector lies within the center-unstable eigenspace of the equilibrium, where the end vector lies within the center-stable eigenspace and where ϵ_0 and ϵ_1 are small, so the continuation of HSN orbits can be started.

4.1.3 Implementation in MATCONT. Analogous notation as for HHS orbits is used. In the Type menu in the MATCONT window, the notations ConnectionSaddleNode and HomotopySaddleNode are used. In the MatCont window, the curve of the time-integration is `LP_ConnecHSN` and `ConnecHSN_HTHSN`, `HTHSN_HTHSN` and `HTHSN_HSN` are the possible continuations. The Starter windows are similar to the Starters used in the homotopy method for HHS orbits, except that in the Starter of `LP_ConnecHSN` only UParam1 has to be filled in by the user, since the starting vector lies in the direction of the eigenvector corresponding to the zero eigenvalue.

We give an example of the method in Section 6.3.

4.2 Starting by Homotopy: Heteroclinic Orbits

4.2.1 The Method. An analogous homotopy method for heteroclinic orbits is also implemented. Let

$$\Re(\mu_{n_S}) \leq \cdots \leq \Re(\mu_1) < 0 < \Re(\lambda_1) \leq ... \leq \Re(\lambda_{n_U}),$$

where $\lambda_1, ..., \lambda_{n_U}$ are the eigenvalues of $f_x(x_0, \alpha)$ with nonnegative real part and $\mu_1, ..., \mu_{n_S}$ are the eigenvalues of $f_x(x_1, \alpha)$ with non-positive real part (with $x(t) \to x_0$

as $t \to -\infty$ and $x(t) \to x_1$ as $t \to +\infty$). The defining system for the continuation of heteroclinic orbits is given by

$$\begin{aligned}
&\dot{x}_C - 2Tf(x_C, \alpha) = 0,\\
&f(x_0, \alpha) = 0,\\
&f(x_1, \alpha) = 0,\\
&\textstyle\int_0^1 \dot{\tilde{x}}^*(t)[x(t) - \tilde{x}(t)]dt = 0,\\
&Q^{U^\perp,\mathrm{T}}(x(0) - x_0) = 0,\\
&Q^{S^\perp,\mathrm{T}}(x(1) - x_1) = 0,\\
&T_{22U}Y_U - Y_U T_{11U} + T_{21U} - Y_U T_{12U} Y_U = 0,\\
&T_{22S}Y_S - Y_S T_{11S} + T_{21S} - Y_S T_{12S} Y_S = 0,\\
&\left\|x(0) - x_0\right\| - \epsilon_0 = 0,\\
&\left\|x(1) - x_1\right\| - \epsilon_1 = 0,
\end{aligned} \tag{18}$$

where $Q^{U^\perp} \in \mathbb{R}^{n\times(n-n_U)}$, $Q^{S^\perp} \in \mathbb{R}^{n\times(n-n_S)}$, $Y_U \in \mathbb{R}^{(n-n_U)\times n_U}$, $Y_S \in \mathbb{R}^{(n-n_S)\times n_S}$. If the phase condition is added, two of the three heteroclinic parameters $T, \epsilon_0, \epsilon_1$ are needed, otherwise only one heteroclinic parameter is needed. We remark that without phase condition in (18) the number of constraints equals $Nmn+4n-n_U-n_S+2+(n-n_U)n_U+(n-n_S)n_S$ and the free scalar variables are given by $x_M, x_0, x_1, \alpha_1, \ldots, \alpha_{n_\alpha-1}, T, Y_U, Y_S$ so that $n_v = Nmn+3n+n_\alpha+(n-n_U)n_U+(n-n_S)n_S$. If the phase condition is added, the number of constraints is augmented by one and an extra heteroclinic parameter has to be freed. For continuation, another parameter has to be freed. Since for continuation $n_c - n_v$ has to be equal to -1, we can conclude that the number of free system parameters has to be equal to $n_\alpha = n - (n_U + n_S) + 2$.

The method is very similar to the homotopy method for HHS orbits. Remark that since we have two different equilibria, in the first step ϵ_1 not necessarily starts increasing anymore. But again, generally, we stop time integration or continuation when ϵ_1 stops decreasing. The algorithm is described in detail in the appendix.

Analogous notation as for HHS and HSN homoclinic orbits is used. The curve of the time-integration is `EP_ConnecHet` and the possible continuations are denoted as `ConnecHet_HTHet`, `HTHet_HTHet`, `HTHet_Het`. The full notations in the Type menu are given by ConnectionHet and HomotopyHet. The Starter windows are similar to the Starters used in the homotopy method for HHS orbits, except that in the Starter of `EP_ConnecHet` $x_0^{(0)}$ and $x_1^{(0)}$ has to be filled in by the user.

We give an example of the method in Section 6.4.

5. DETECTION OF CODIM 2 GLOBAL HOMOCLINIC BIFURCATIONS

Relationships between homoclinic objects of codimension 1 and 2 computed by MATCONT are presented in Figure 2, while the symbols and their meaning are summarized in Table I.

The arrows in Figure 2 have the following meaning. In general, an arrow from an object of type A to an object of type B means that that object of type B can be detected (either automatically or by inspecting the output) during the computation of a curve of objects of type A. '*' stands for either S or U, depending on whether a stable or an unstable invariant manifold is involved.

During HSN continuation, only one bifurcation is tested for, namely the non-central homoclinic-to-saddle-node orbit or NCH orbit. This orbit forms the transition between HHS and HSN curves. The strategy used for detection is taken from HomCont

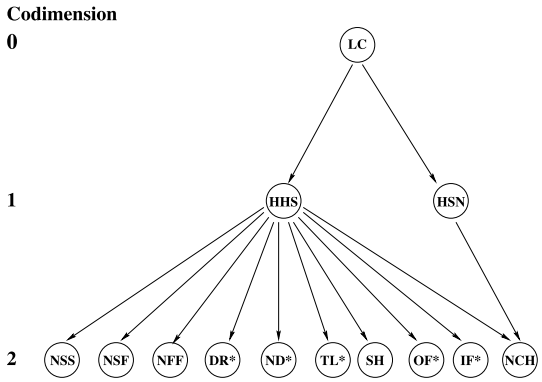

Fig. 2. The graph of adjacency for homoclinic bifurcations in MATCONT; here * stands for S or U.

Table I. Objects Related to Homoclinics to Equilibria and Their Labels within the GUI

Type of object	Label
Limit cycle	LC
Homoclinic to Hyperbolic Saddle	HHS
Homoclinic to Saddle-Node	HSN
Neutral saddle	NSS
Neutral saddle-focus	NSF
Neutral Bi-Focus	NFF
Shilnikov-Hopf	SH
Double Real Stable leading eigenvalue	DRS
Double Real Unstable leading eigenvalue	DRU
Neutrally-Divergent saddle-focus (Stable)	NDS
Neutrally-Divergent saddle-focus (Unstable)	NDU
Three Leading eigenvalues (Stable)	TLS
Three Leading eigenvalues (Unstable)	TLU
Orbit-Flip with respect to the Stable manifold	OFS
Orbit-Flip with respect to the Unstable manifold	OFU
Inclination-Flip with respect to the Stable manifold	IFS
Inclination-Flip with respect to the Unstable manifold	IFU
Non-Central Homoclinic to saddle-node	NCH

[Champneys et al. 1996]. There are two kinds of NCH orbits, one concerns the unstable direction, one the stable direction; the testfunctions are respectively given by

$$\psi_1 = \frac{1}{T}\langle x(0) - x_0,\, p\rangle,$$
$$\psi_2 = \frac{1}{T}\langle x(1) - x_0,\, p\rangle,$$

with p a unit left singular vector of A. As test function for an NCH bifurcation in MATCONT, only one test function is used, namely the product of ψ_1 and ψ_2.

During HHS continuation, all bifurcations detected in HomCont are also detected in our implementation. For this, mostly test functions from Champneys et al. [1996] are used.

The test functions for the bifurcations are:

— Neutral saddle, saddle-focus or bi-focus

$$\psi = \Re(\mu_1) + \Re(\lambda_1)$$

If both μ_1 and λ_1 are real, then it is a neutral saddle, if one is real and one consists of a pair of complex conjugates, the bifurcation is a saddle-focus, and it is a bi-focus when both eigenvalues consist of a pair of complex conjugates.

— Double real stable leading eigenvalue

$$\psi = \begin{cases} (\Re(\mu_1) - \Re(\mu_2))^2, \Im(\mu_1) = 0 \\ -(\Im(\mu_1) - \Im(\mu_2))^2, \Im(\mu_1) \neq 0 \end{cases}$$

— Double real unstable leading eigenvalue

$$\psi = \begin{cases} (\Re(\lambda_1) - \Re(\lambda_2))^2, \Im(\lambda_1) = 0 \\ -(\Im(\lambda_1) - \Im(\lambda_2))^2, \Im(\lambda_1) \neq 0 \end{cases}$$

— Neutrally divergent saddle-focus (stable)

$$\psi = \Re(\mu_1) + \Re(\mu_2) + \Re(\lambda_1)$$

— Neutrally divergent saddle-focus (unstable)

$$\psi = \Re(\mu_1) + \Re(\lambda_2) + \Re(\lambda_1)$$

— Three leading eigenvalues (stable)

$$\psi = \Re(\mu_1) - \Re(\mu_3)$$

— Three-leading eigenvalues (unstable)

$$\psi = \Re(\lambda_1) + \Re(\lambda_3)$$

— Noncentral homoclinic-to-saddle-node

$$\psi = \Re(\mu_1)$$

— Shil'nikov-Hopf

$$\psi = \Re(\lambda_1)$$

— Bogdanov-Takens point

$$\psi = \begin{cases} \Re(\mu_1) \\ \Re(\lambda_1) \end{cases}$$

We now investigate the orbit- and inclination-flip bifurcations. It is possible to choose normalized eigenvectors p_1^s and p_1^u of $A^{\mathrm{T}}(x_0, \alpha_0)$ and q_1^s and q_1^u of $A(x_0, \alpha_0)$ depending smoothly on (x_0, α_0), which satisfy

$$A^{\mathrm{T}}(x_0, \alpha_0)\, p_1^s = \mu_1\, p_1^s \qquad A^{\mathrm{T}}(x_0, \alpha_0)\, p_1^u = \lambda_1\, p_1^u$$
$$A(x_0, \alpha_0)\, q_1^s = \mu_1\, q_1^s \qquad A(x_0, \alpha_0)\, q_1^u = \lambda_1\, q_1^u.$$

If μ_1 and/or λ_1 is/are complex, we also have

$$A^{\mathrm{T}}(x_0, \alpha_0)\, \overline{p}_1^s = \overline{\mu}_1\, \overline{p}_1^s \qquad A^{\mathrm{T}}(x_0, \alpha_0)\, \overline{p}_1^u = \overline{\lambda}_1\, \overline{p}_1^u$$
$$A(x_0, \alpha_0)\, \overline{q}_1^s = \overline{\mu}_1\, \overline{q}_1^s \qquad A(x_0, \alpha_0)\, \overline{q}_1^u = \overline{\lambda}_1\, \overline{q}_1^u.$$

The test functions for the orbit-flip bifurcations are then:

— Orbit-flip with respect to the stable manifold

$$\psi = \begin{cases} e^{-\Re(\mu_1)T}\langle \Re(p_1^s), x(1) - x_0\rangle \\ e^{-\Re(\mu_1)T}\langle \Im(p_1^s), x(1) - x_0\rangle \end{cases}$$

if $\mu_1 \in \mathbb{C}$. In the case, that $\mu_1 \in \mathbb{R}$, we use twice the first testfunction (in the MATCONT-environment it is not feasible to have different numbers of test functions for the same bifurcation).

— Orbit-flip with respect to the unstable manifold

$$\psi = \begin{cases} e^{\Re(\lambda_1)T}\langle \Re(p_1^u), x(0) - x_0\rangle \\ e^{\Re(\lambda_1)T}\langle \Im(p_1^u), x(0) - x_0, \rangle \end{cases}$$

if $\lambda_1 \in \mathbb{C}$. In the case that $\lambda_1 \in \mathbb{R}$, we use twice the first testfunction (same reason as before).

For the inclination-flip bifurcations, the following test functions are introduced:

— Inclination-flip with respect to the stable manifold

$$\psi = \begin{cases} e^{-\Re(\mu_1)T}\langle \Re(q_1^s), \phi(0)\rangle \\ e^{-\Re(\mu_1)T}\langle \Im(q_1^s), \phi(0)\rangle \end{cases}$$

if $\mu_1 \in \mathbb{C}$. In the case that $\mu_1 \in \mathbb{R}$, we use twice the first testfunction (same reason as before).

— Inclination-flip with respect to the unstable manifold

$$\psi = \begin{cases} e^{\Re(\lambda_1)T}\langle \Re(q_1^u), \phi(1)\rangle \\ e^{\Re(\lambda_1)T}\langle \Im(q_1^u), \phi(1)\rangle \end{cases}$$

if $\lambda_1 \in \mathbb{C}$. In the case that $\lambda_1 \in \mathbb{R}$, we use twice the first testfunction (same reason as before).

In this case, $\phi \in \mathcal{C}^1([0, 1], \mathbb{R}^n)$ is the solution to the adjoint system:

$$\begin{cases} \dot{\phi}(t) + 2TA^{\mathrm{T}}(x(t), \alpha_0)\phi(t) = 0 \\ Q^{S,\mathrm{T}}\phi(1) = 0 \\ Q^{U,\mathrm{T}}\phi(0) = 0 \\ \int_0^1 \widetilde{\phi}^{\mathrm{T}}(t)[\phi(t) - \widetilde{\phi}(t)]dt = 0, \end{cases} \tag{19}$$

where, as before, Q^S and Q^U are matrices whose columns form bases for the stable and unstable eigenspaces of $A(x_0, \alpha_0)$, respectively, and the last condition selects one solution out of the family $c\phi(t)$ for $c \in \mathbb{R}$.

However, it is possible to compute the previously-mentioned test functions in a more efficient way, without having to explicitly find the solution ϕ to the adjoint system.

PROPOSITION 5.1. *If ϕ is a solution to* (19) *and $\zeta_1 \in \mathbb{R}^{n_U}$, $\zeta_2 \in \mathbb{R}^{n_S}$, then*

$$\begin{pmatrix} \phi(t) \\ \zeta_1 \\ \zeta_2 \end{pmatrix} \perp \mathit{Range} \begin{pmatrix} D - 2TA(x(t), \alpha_0) \\ Q^{S^\perp,\mathrm{T}} \delta(1) \\ Q^{U^\perp,\mathrm{T}} \delta(0) \end{pmatrix} \tag{20}$$

$$\Longleftrightarrow$$

$$\begin{cases} Q^{S^\perp} \zeta_1 = -\phi(1) \\ Q^{U^\perp} \zeta_2 = \phi(0). \end{cases} \tag{21}$$

Here D and δ are the differentiation and the evaluation operator, respectively, and $Q^{S^\perp}$ and $Q^{U^\perp}$ are the orthogonal complements of Q^S and Q^U, respectively.

PROOF. The necessary and sufficient condition is that for all $g \in \mathbb{C}^1([0, 1], \mathbb{R}^n)$

$$\begin{pmatrix} \phi(t) \\ \zeta_1 \\ \zeta_2 \end{pmatrix} \perp \begin{pmatrix} \dot{g}(t) - 2TA(x(t), \alpha_0) g(t) \\ Q^{S^\perp,\mathrm{T}} g(1) \\ Q^{U^\perp,\mathrm{T}} g(0) \end{pmatrix},$$

that is,

$$\begin{aligned} &\int_0^1 \phi(t)^\mathrm{T} (\dot{g}(t) - 2TA(x(t), \alpha_0) g(t)) dt + \zeta_1^\mathrm{T} Q^{S^\perp,\mathrm{T}} g(1) + \zeta_2^\mathrm{T} Q^{U^\perp,\mathrm{T}} g(0) = 0 \\ \Longleftrightarrow\ &\left[\phi(t)^\mathrm{T} g(t)\right]_0^1 - \int_0^1 (\dot{\phi}(t)^\mathrm{T} g(t) + 2T\phi(t)^\mathrm{T} A(x(t), \alpha_0) g(t)) dt \\ &\quad + \zeta_1^\mathrm{T} Q^{S^\perp,\mathrm{T}} g(1) + \zeta_2^\mathrm{T} Q^{U^\perp,\mathrm{T}} g(0) = 0, \end{aligned}$$

where

$$\begin{aligned} &\dot{\phi}(t)^\mathrm{T} g(t) + 2T\phi(t)^\mathrm{T} A(x(t), \alpha_0) g(t) \\ &\qquad = g(t)^\mathrm{T} \left(\dot{\phi}(t)^\mathrm{T} + 2TA^\mathrm{T}(x(t), \alpha_0)\phi(t)\right) \\ &\qquad = 0. \end{aligned}$$

So the necessary and sufficient condition is

$$\begin{aligned} &\phi(1)^\mathrm{T} g(1) - \phi(0)^\mathrm{T} g(0) + \zeta_1^\mathrm{T} Q^{S^\perp,\mathrm{T}} g(1) + \zeta_2^\mathrm{T} Q^{U^\perp,\mathrm{T}} g(0) = 0 \\ \Longleftrightarrow\ &(\phi(1)^\mathrm{T} + \zeta_1^\mathrm{T} Q^{S^\perp,\mathrm{T}}) g(1) - (\phi(0)^\mathrm{T} - \zeta_2^\mathrm{T} Q^{U^\perp,\mathrm{T}}) g(0) = 0. \end{aligned}$$

This must hold for all g, hence

$$\begin{cases} \zeta_1^\mathrm{T} Q^{S^\perp,\mathrm{T}} = -\phi(1)^\mathrm{T} \\ \zeta_2^\mathrm{T} Q^{U^\perp,\mathrm{T}} = \phi(0)^\mathrm{T} \end{cases}$$

or

$$\begin{cases} Q^{S^\perp} \zeta_1 = -\phi(1) \\ Q^{U^\perp} \zeta_2 = \phi(0). \end{cases}$$

□

We note that by (19) $\phi(1)$ and $\phi(0)$ are vectors, orthogonal to the stable and unstable eigenspaces, respectively, so (21) is solvable. In fact, the solutions are unique since $Q^{S^\perp}$ and $Q^{U^\perp}$ are full rank matrices.

Thus, ζ_1 and ζ_2 are determined uniquely, so that the test functions for inclination-flip can be rewritten as

— Inclination-flip with respect to the stable manifold

$$\psi = \begin{cases} \langle \Re(q_1^s), \boldsymbol{Q}^{U^\perp} \zeta_2 \rangle \\ \langle \Im(q_1^s), \boldsymbol{Q}^{U^\perp} \zeta_2 \rangle \end{cases}$$

if $\mu_1 \in \mathbb{C}$. In the case that $\mu_1 \in \mathbb{R}$, we use twice the first test function. The factor $e^{-\Re(\mu_1)T}$ is now omitted since the inproduct is already normalized.

— Inclination-flip with respect to the unstable manifold

$$\psi = \begin{cases} -\langle \Re(q_1^u), \boldsymbol{Q}^{S^\perp} \zeta_1 \rangle \\ -\langle \Im(q_1^u), \boldsymbol{Q}^{S^\perp} \zeta_1 \rangle \end{cases}$$

if $\lambda_1 \in \mathbb{C}$. In the case that $\lambda_1 \in \mathbb{R}$, we use twice the first testfunction. The factor $e^{\Re(\lambda_1)T}$ is omitted since the inproduct is already normalized.

These test functions are very efficiently computable: $\boldsymbol{Q}^{U^\perp}$ and $\boldsymbol{Q}^{S^\perp}$ are already computed during the homoclinic continuation, for the continuation of the invariant subspaces; μ_1, λ_1, q_1^s and q_1^u are also already known. The only quantities that seem harder to compute are ζ_1 and ζ_2.

But the advantage of our computation becomes clear when comparing the matrix in (20) to the equations (2) and (10), which are part of the defining system for HHS orbits. Indeed, the big matrix in the discretization of (20) is for a major part identical to the Jacobian matrix used during homoclinic continuation, and therefore almost no extra time is required to compute it. After selecting the necessary rows and columns from the already computed Jacobian, the resulting matrix is bordered with its left and right singular vectors, which results in a nonsingular matrix (call it B). Then, solving $B^{\mathrm{T}}\psi = [\,0\ \cdots\ 0\ 1\,]^{\mathrm{T}}$ results in finding ζ_1 and ζ_2 as two- and one-but-last block elements of the vector ψ. This vector is also the new left singular vector of B, after eliminating the last element and normalizing the vector. Similarly, the new right singular vector can be found by solving $B\Phi = [\,0\ \cdots\ 0\ 1\,]^{\mathrm{T}}$, removing the last element and renormalizing Φ. Thus, our algorithm, while computing ζ_1 and ζ_2 relatively cheaply, also keeps track of the singular vectors which facilitate getting a well-conditioned matrix B.

An example of an inclination-flip bifurcation is given in Section 6.5.

6. EXAMPLES

6.1 HHS Orbits in the Lorenz System

One of the best-known dynamical systems with orbits homoclinic to an equilibrium point is the three-dimensional system [Lorenz 1963], given by

$$\begin{cases} \dot{x} = \sigma(y - x), \\ \dot{y} = rx - y - xz, \\ \dot{z} = -bz + xy, \end{cases} \tag{22}$$

with the standard values $\sigma = 10$, $b = 8/3$, and where r is the primary bifurcation parameter. With these parameter values, a supercritical pitchfork bifurcation from

the trivial equilibrium occurs at $r = 1$, giving rise to two symmetric nontrivial equilibria. At approximately $r = 13.926$, there are two symmetry-related orbits that are homoclinic to the origin, and from which two primary families of saddle cycles arise (together with a nontrivial hyperbolic invariant set containing many other periodic and nonperiodic orbits). One of these homoclinic orbits is located entirely in the half-space $x > 0$ and has one maximum of the x-component of its solution. We will refer to this orbit as the $(1, 0)$-loop and say that it makes one turn around the corresponding nontrivial equilibrium. It is well known that - at other parameter values - the Lorenz system has homoclinic orbits with one positive maximum and n negative minima of the x-component of the corresponding solution. Such homoclinic orbits make one turn around the nontrivial equilibrium with $x > 0$ and n turns around the nontrivial equilibrium with $x < 0$. We will call these orbits the $(1, n)$-loops, following Petrovskaya and Judovich [1980].

Our aim here is to illustrate how one can compute bifurcation values of parameter r at which $(1, n)$-loops exist and how to continue the corresponding bifurcation curves in the (σ, r)-plane with MATCONT. Note that the number of turns n can change along a homoclinic bifurcation curve. In particular, we will compute (a segment of) a homoclinic bifurcation curve that spirals towards the so called T-point $(\sigma_\infty, r_\infty) \approx (10.16, 30.87)$, where the Lorenz system has a codimension 2 heteroclinic orbit connecting the trivial and nontrivial equilibria. Along this curve, n goes to infinity when we approach the T-point. This codim 2 global bifurcation has been analyzed in detail by Bykov [1978, 1980] and later rediscovered by Glendinning and Sparrow [1986].

To begin with, fix $r = 15.5$. Then, the origin is a saddle equilibrium of (22) with eigenvalues

$$\lambda_1^{(0)} = 7.7382, \quad \mu_1^{(0)} = -2.6667, \quad \mu_2^{(0)} = -18.7382$$

and the normalized unstable eigenvector corresponding to $\lambda_1^{(0)} > 0$ equals

$$q_{0,1}^{(0)} = \begin{pmatrix} -0.4911 \\ -0.8711 \\ 0 \end{pmatrix}.$$

Since we want to compute homoclinic orbits departing from the origin in the half-space $x > 0$, we take UParam1 $= -1$. Then, we integrate the orbit starting at distance $\epsilon_0 = 0.01$ from the origin over time interval $T = 1.3$ by computing in MATCONT the `EP_ConnecHom` curve. The integration produces the orbit segment shown in Figure 3(a) that is far from being homoclinic but is sufficient to start the homotopy method.

By selecting the connection in the Starter window, we are automatically prepared to compute the `ConnecHom_HTHom` curve. In this continuation, where we use 20 mesh intervals, the system parameter r, as well as SParam1 and ϵ_1 are active. The initial values of these last two parameters are Sparam1 $= -0.0668$ and $\epsilon_1 = 18.5152$, respectively. While SParam1 indicates that the end-point of the integrated orbit is rather close to the plane tangent to the 2D-stable invariant manifold of the origin, its distance ϵ_1 to the equilibrium is quite large. The continuation produces a family of orbit segments attaining SParam1 $= 0$ at $r = 16.1793$ (Figure 3(b)), where $\epsilon_1 = 17.4523$.

Selecting the last point as initial point for the next continuation, we can compute the `HTHom_HTHom` curve with r, T and ϵ_1 as active parameters (note that now T is set to 0.65, that is one-half of its initial value). Our goal at this stage is to reach $\epsilon_1 = 0.5$ by increasing the interval T. This indeed happens at $T = 1.3476$ with $r = 13.9266$

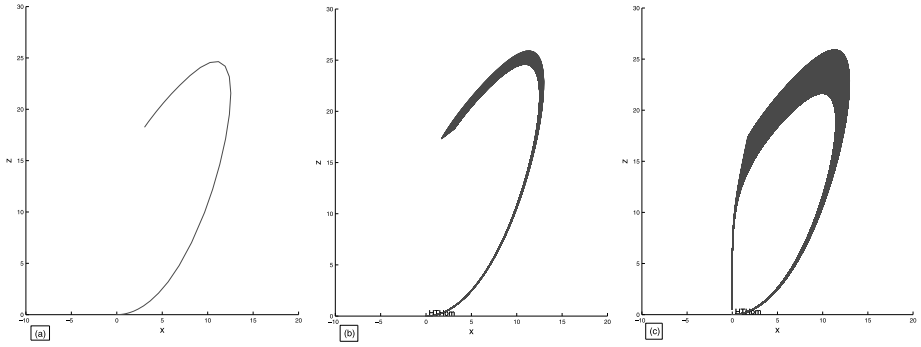

Fig. 3. Initializing the $(1, 0)$-homoclinic orbit by homotopy.

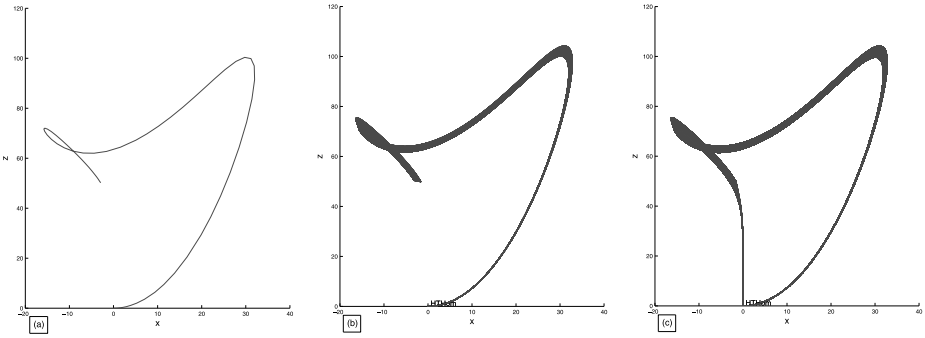

Fig. 4. Initializing the $(1, 1)$-homoclinic orbit by homotopy.

which is a good approximation for the $(1, 0)$-homoclinic parameter value, see Figure 3(c).

After selecting the last point and the curve type `HTHom_Hom`, we are ready to continue the found homoclinic orbit in the two system parameters σ and r, keeping T and ϵ_1 active. It produces the $(1, 0)$-homoclinic curve on Figure 6.

Similar steps, but starting with $r = 55$, produce Figure 4. The initial integration `EP_ConnecHom` with $T = 0.9$ gives Figure 4(a) where Sparam1 = 0.0329 and $\epsilon_1 = 50.3656$. We take a mesh consisting of $N = 40$ intervals and use the standard value $m = 4$. Selecting the last orbit as initial orbit for the continuation of the `ConnecHom_HTHom`-curve with r, SParam1, and ϵ_1 active, gives us Figure 4(b) with SParam1 = 0 at $r = 56.9941$ and $\epsilon_1 = 49.8634$. From this last point, the continuation of the `HTHom_HTHom`-curve is executed with r, T and ϵ_1 free, until $\epsilon_1 = 0.5$. This is obtained at the $(1, 1)$-homoclinic parameter value $r = 54.6460$ and the improved connection is shown in Figure 4(c). Figures 5 and 6 (left) show the family of the $(1, 1)$-homoclinic orbits along the corresponding `HTHom_Hom`-curve.

Figure 6 includes results of similar computations for the $(1, n)$-homoclinic curves with various n, obtained with the same homotopy method. The $(1, \infty)$-curve spirals towards the T-point previously mentioned; along this curve, the homoclinic orbit approaches the heteroclinic cycle connecting the origin to the nontrivial equilibrium and from this equilibrium back to the origin. Most of the curves in Figure 6 were first reported in Petrovskaya and Judovich [1980]; we present several more of them with the main purpose to illustrate the power of MATCONT that allows to produce such figures in a matter of minutes. The continuation took 22.2 seconds to compute 100

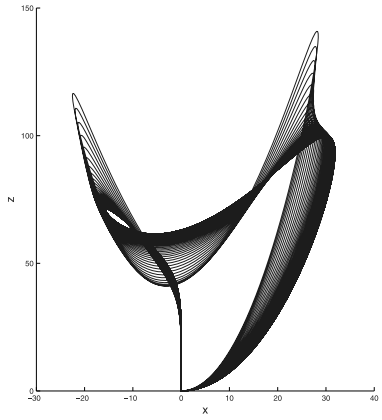

Fig. 5. A family of $(1, 1)$-homoclinic orbits.

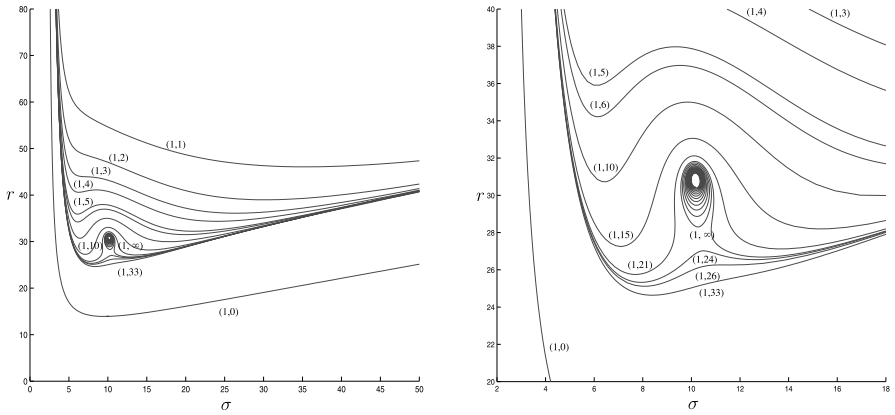

Fig. 6. Partial two-parameter bifurcation diagram of the Lorenz system and its magnification near the T-point.

$(1, 0)$-homoclinic orbits. The runs were executed in MatLab version 7.5.0, on an Intel 2.99-GHz machine with 1.99-Gigabyte RAM. We also stress that the figure shows only a small portion of the (σ, r)-bifurcation diagram of the Lorenz system, even if one is concerned only with homoclinic bifurcations. For example, there are sequences of T-points corresponding to different heteroclinic contours, with their own homoclinic spirals.

6.2 HHS Orbits in Hopf-Hopf Normal Form with Broken Symmetry

We consider the normal form of the Hopf-Hopf codimension-2 bifurcation in polar coordinates:

$$\begin{cases} \dot{r_1} = r_1(\mu_1 + p_{11}r_1^2 + p_{12}r_2^2 + s_1r_2^4) \\ \dot{r_2} = r_2(\mu_2 + p_{21}r_1^2 + p_{22}r_2^2 + s_2r_1^4) \\ \dot{\varphi_1} = \omega_1 \\ \dot{\varphi_2} = \omega_2. \end{cases}$$

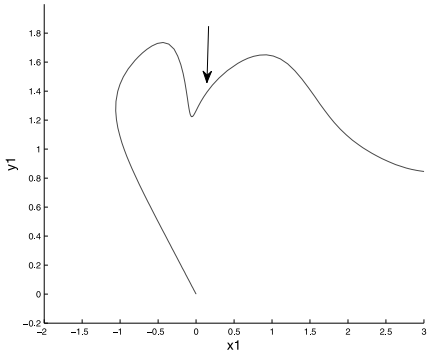

Fig. 7. Starting orbit after time integration.

We rewrite this system in the cartesian (x_1, y_1, x_2, y_2)-coordinates and add an order 6 term so that we obtain the following equations:

$$\begin{cases} \dot{x_1} = x_1(\mu_1 + p_{11}(x_1^2 + y_1^2) + p_{12}(x_2^2 + y_2^2) + s_1(x_2^2 + y_2^2)^2) - y_1\omega_1 + \mathbf{3y_1^6} \\ \dot{y_1} = y_1(\mu_1 + p_{11}(x_1^2 + y_1^2) + p_{12}(x_2^2 + y_2^2) + s_1(x_2^2 + y_2^2)^2) + x_1\omega_1 - \mathbf{2x_2^6} \\ \dot{x_2} = x_2(\mu_2 + p_{21}(x_1^2 + y_1^2) + p_{22}(x_2^2 + y_2^2) + s_2(x_1^2 + y_1^2)^2) - y_2\omega_2 - \mathbf{7y_1^6} \\ \dot{y_2} = y_2(\mu_2 + p_{21}(x_1^2 + y_1^2) + p_{22}(x_2^2 + y_2^2) + s_2(x_1^2 + y_1^2)^2) + x_2\omega_2 + \mathbf{x_1^6}. \end{cases}$$

The initial parameter values are: $\mu_1 = 9.7, \mu_2 = -50, p_{11} = 1, p_{12} = 1.5, p_{21} = -2, p_{22} = -1, s_1 = 1.3, s_2 = 1.7, \omega_1 = 0.001, \omega_2 = 0.00235$. The origin is an equilibrium of this system and the eigenvalues are given by $\lambda_1^{(0)} = 9.7 + 0.001i$, $\lambda_2^{(0)} = 9.7 - 0.001i$, $\mu_1^{(0)} = -50 + 0.00235i$, $\mu_2^{(0)} = -50 - 0.00235i$; so we have a two-dimensional unstable manifold and a two-dimensional stable manifold where in both cases the eigenvalues consist of a conjugate complex pair. This gives us an interesting example for the application of the homotopy method.

Since the eigenvalues with smallest positive real part constitute a conjugate complex pair, both UParam1 and UParam2 play a role in the initialization, we set them equal to -1 and 1, respectively. The unstable parameters are now automatically rescaled: UParam1 = -0.7071, UParam2 = 0.7071, and thus UParam1^2 + UParam2^2 = 1. As value of ϵ_0 we take 1.4142e-4. Therefore, we start time integration from the point

$$x(0) = \begin{pmatrix} 0 \\ 0 \\ 0 \\ 0 \end{pmatrix} + 1.4142\text{e-}4(-0.7071q_{0,1}^{(0)} + 0.7071q_{0,2}^{(0)}),$$

where $q_{0,1}^{(0)} = (1, 0, 0, 0)^{\mathrm{T}}$ and $q_{0,2}^{(0)} = (0, 1, 0, 0)^{\mathrm{T}}$ span the two-dimensional eigenspace corresponding to the eigenvalues $9.7 \pm 0.001i$.

When we execute time-integration over an interval of length 1.1, we obtain Figure 7. First, ϵ_1 increases, then this distance decreases, and then starts to increase again. MATCONT searches for that point where ϵ_1 stops decreasing, which is indicated by the arrow, as endpoint of the initial connecting orbit. None of the stable connection parameters equals zero, however they are quite small; -0.03550 and -0.7491. We now start the successive homotopies where we use a discretization of 50 mesh intervals and 4 collocation points.

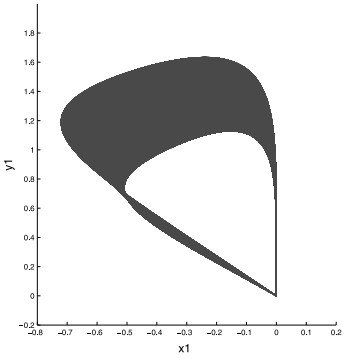

Fig. 8. A family of focus-focus homoclinic orbits.

Doing the continuation with both unstable and both stable connection parameters and ϵ_1 free, SParam1 becomes zero and SParam2 equals -0.7472. To make this last stable connection parameter zero, a system parameter has to be varied, we take μ_2. This gives $\epsilon_1 = 1.2490$, so a continuation, with T, ϵ_1 and μ_2 free, is needed to decrease ϵ_1. We put eps1tol equal to 0.0001, and ϵ_1 reaches this value for $T = 0.8299$ and $\mu_2 = -14.3953$. A family of homoclinic orbits originating at this end orbit is given in Figure 8, where T and ϵ_1 are the free homoclinic parameters and μ_1 and μ_2 the free system parameters. The continuation of 100 HHS orbits took 118.6 seconds. The runs were executed in MATLAB version 7.5.0, on an Intel 2.99-GHz machine with 1.99-Gigabyte RAM.

In this example, we also want to pay some attention to the comparison of the Riccati equations and the method of Beyn et al. [2001] for the continuation of the invariant subspaces. The condition numbers of the Jacobian were very similar. Let's therefore focus on the speed. The continuation which makes SParam1 zero took 11.8 seconds with the Riccati equations and 10.9 seconds with the method of Beyn et al. To find the zero of SParam2, 17.9 seconds were needed against 20.2 with the method of Beyn et al. [2001]. The third homotopy step lasted 231.2 seconds against 244.2 seconds. And the continuation of 100 homoclinic orbits took 118.6 seconds when using the Riccati equations while it took 116.1 seconds when using the method proposed in Beyn et al. [2001].

6.3 HSN Orbits in a Cell Cycle Model

As example of the homotopy method for HSN orbits, we study the following cell cycle model:

$$\begin{cases} \dot{X} = k_1 - (k_2' + k_2'' Y)X, \\ \dot{Y} = \frac{(k_3' + k_3'' A)(1-Y)}{J_3 + 1 - Y} - \frac{k_4 m X Y}{J_4 + Y}, \\ \dot{A} = k_5' + k_5'' \frac{(mX)^n}{J_5^n + (mX)^n} - k_6 A, \end{cases}$$

introduced in Tyson and Novak [2001]. A continuum of HSN orbits was computed in Govaerts et al. [2009] where the continuation was started up from a limit cycle of large period. During this continuation a non-central homoclinic to saddle-node orbit was detected. We now recompute these orbits, starting from the limit point $x_0^{(0)} = (0.0461, 0.8269, 0.0504)^{\mathrm{T}}$ where the initial parameter values are given by: $k_1 = 0.04, k_2' = 0.04, k_2'' = 1, k_3' = 1, k_3'' = 10, k_4 = 35, J_3 = 0.04, J_4 = 0.04, k_5' = 0.005, k_5'' = 0.2, k_6 = 0.1, J_5 = 0.3, n = 4, m = 0.7933$. The eigenvalues in $x_0^{(0)}$ are $\nu_1^{(0)} = 8.9930\text{e-}7$, $\mu_1^{(0)} = -9.3355\text{e-}2$, $\mu_2^{(0)} = -2.2666$, so $n_U = 0$.

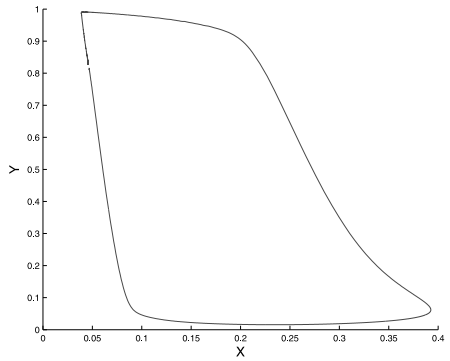

Fig. 9. Starting orbit after time integration.

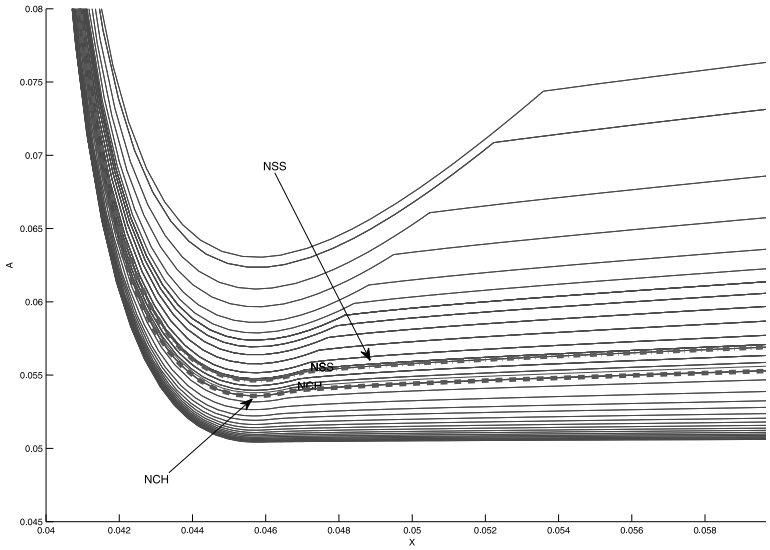

Fig. 10. Continuum of HHS orbits and HSN orbits which converge to the NCH orbit.

Figure 9 shows the orbit obtained by time integration from $x_0^{(0)}$ with UParam1 = 1 and $\epsilon_0 = 0.01$ over an interval of length 200. This is clearly a proper starting orbit so the successive homotopies can be executed. For discretization, we use 50 mesh intervals and 4 collocation points. Since there are no strictly positive eigenvalues, no τ's have to be made zero, so we can immediately execute the continuation which makes ϵ_1 small. Although, ϵ_1 is already very small, namely 0.0036, we do the continuation until T and ϵ_1 are given by 1445.6988 and $1e{-}4$, respectively. The continuation of HSN orbits can now be started, with ϵ_0 and ϵ_1 as free homoclinic parameters, and k_4 and m as free system parameters. The continuation works well and the NCH orbit is detected. The continuation of 100 HSN orbits took 79.3 seconds, with the same computer specifications as previously mentioned.

The HSN orbits that converge to the NCH orbit are the lower orbits in Figure 10. But the NCH orbit can also be detected on a branch of HHS orbits which approach from the opposite direction. After a neutral saddle bifurcation, the HHS orbits disappear when encountering the NCH orbit where $k_4 = 21.294025$ and $m = 1.3309616$.

6.4 Heteroclinic Orbits in a Model of the Josephson Junction

We consider the 3D Josephson Junction problem, introduced in Doedel et al. [1994]:

$$\begin{cases} \dot{x} = y, \\ \dot{y} = z, \\ \dot{z} = ((1-c^2)z + \alpha c\, y - \sin(x) + \gamma)/(\beta c). \end{cases}$$

This system contains the two equilibria $x_0^{(0)} = (\arcsin(\gamma), 0, 0)^{\mathrm{T}}$ and $x_1^{(0)} = (\pi - \arcsin(\gamma), 0, 0)^{\mathrm{T}}$. Consider the parametervalues $\alpha = 0.18, \beta = 0.1, \gamma = 0.1, c = 0.6$, where $x_0^{(0)} = (0.1002, 0, 0)^{\mathrm{T}}$ and $x_1^{(0)} = (3.0414, 0, 0)^{\mathrm{T}}$. The eigenvalues in $x_0^{(0)}$ and $x_1^{(0)}$ are given by

$$\begin{pmatrix} 10.6899 \\ 1.2339 \\ -1.2572 \end{pmatrix} \quad \text{and} \quad \begin{pmatrix} 10.9686 \\ -0.1510 + 1.2203i \\ -0.1510 - 1.2203i \end{pmatrix},$$

respectively. We have a two-dimensional unstable manifold in $x_0^{(0)}$, where the eigenvalue with smallest positive real part is real so only the first unstable connection parameter has to be taken into account in the first step, and a two-dimensional stable manifold in $x_1^{(0)}$. This gives us two unstable connection parameters and one stable connection parameter. The starting point is $x(0) = x_0^{(0)} + \epsilon_0 \mathrm{UParam1} q_{0,1}^{(0)}$ with $q_{0,1}^{(0)} = (-0.4545, -0.5608, -0.6920)^{\mathrm{T}}$, the eigenvector corresponding to eigenvalue 1.2339. We initialize UParam1 $= -1$ and $\epsilon_0 = 0.0001$ and do time integration over an interval of length 3. MATCONT takes that part of the time-integrated orbit up to the point where ϵ_1 stops decreasing, which in this case is only a very small segment, where SParam1 $= -0.8175$.

In the successive homotopies, we use a discretization with 50 mesh intervals and 4 collocation points. A continuation with all the connection parameters and ϵ_1 free, places the end-vector $x(1) - x_1^{(0)}$ in the stable eigenspace of $x_1^{(0)}$, the end-value of ϵ_1 equals 5.1783. Note that $n_\alpha = n - (n_U + n_S) + 2 = 3 - (2+2) + 2 = 1$, so in the continuation to make ϵ_1 small, no free system parameters are needed.

A plot of this continuation is given in Figure 11. The initial orbit is the small vertical line on the left and the homotopy steps lead to a proper starting orbit for the computation of a branch of heteroclinic orbits. This gives us an indication of the robustness of the method. The stable eigenspace of $x_1^{(0)}$ is two-dimensional, namely we have a conjugate complex pair of eigenvalues with negative real part, which explains the spiral convergence to $x_1^{(0)}$ as can be seen in the figure. The end-values of the heteroclinic parameters are $T = 30.4026$ and $\epsilon_1 = 0.0001$. Finally, we can start the continuation of heteroclinic orbits, taking c as free system parameter and T as free heteroclinic parameter. The result is shown in Figure 12. The continuation of 100 heteroclinic orbits took 49.7 seconds.

6.5 An Inclination Flip in the Shimizu-Morioka Equations

In our last example, we consider the inclination-flip bifurcation, appearing in the following Shimizu-Morioka model [Champneys and Kuznetsov 1994]:

$$\begin{cases} \dot{x} = y, \\ \dot{y} = \kappa y - \lambda x - xz, \\ \dot{z} = -z + x^2. \end{cases}$$

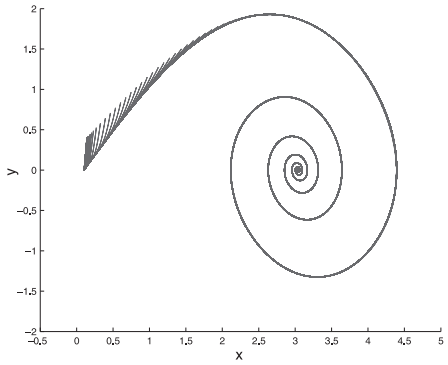

Fig. 11. Continuation which makes ϵ_1 small.

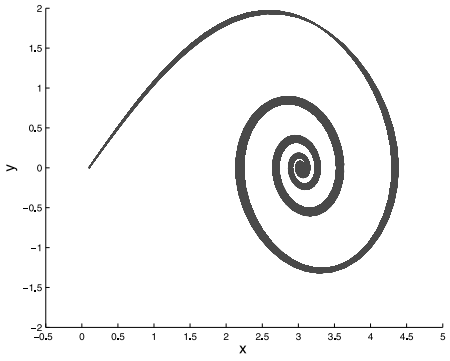

Fig. 12. A family of heteroclinic orbits.

We start time integration from a point close to the equilibrium $(0, 0, 0)^{\mathrm{T}}$, with parametervalues $(\kappa, \lambda) = (-1, -3)$. This gives us a closed orbit from which the continuation of periodic orbits can be started, with κ and T free. The period increases very quickly while the parametervalue remains nearly constant at $\kappa = -1.079$. A homoclinic orbit is found, we take ϵ_0 and ϵ_1 as free homoclinic parameters for the continuation. An inclination-flip with respect to the stable manifold occurs at $(\kappa, \lambda) = (-1.087755740270267, -3.101548085292658)$, the homoclinic orbit is given in Figure 13. The eigenvalues are $1.2993, -2.3871$ and -1 so we have two times the same testfunction. The continuation of 100 HHS orbits took 65.3 seconds, with the same computer specifications as above.

7. DISCUSSION

The current implementation in MATCONT uses the Riccati equations for the continuation of invariant subspaces. Another possibility to keep track of these subspaces is to use an idea proposed in Beyn et al. [2001]. Then, equations of the folllowing type for (Q, Λ) should be used in the defining system for the continuation:

$$\begin{aligned} AQ - Q\Lambda &= 0 \\ Q_0^{\mathrm{T}} Q - I &= 0. \end{aligned} \tag{23}$$

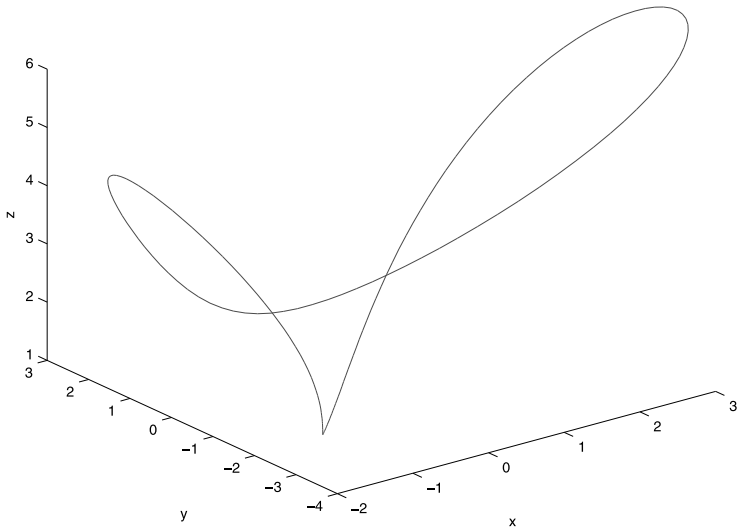

Fig. 13. Homoclinic orbit at the inclination-flip bifurcation.

The columns of $Q \in \mathbb{R}^{n\times d}$ form a basis for the d-dimensional stable or unstable eigenspace (or their orthogonal complements) of A, while $\Lambda \in \mathbb{R}^{d\times d}$ is an auxiliary matrix. The orthogonal matrix Q_0 gives a basis for the appropriate space at the base point.

Both methods have their pros and cons. The method based on (23) is slightly easy to implement but the Jacobian is bigger. We have performed comparison tests in several examples and will here discuss both approaches in the case of the Hopf-Hopf normal form with broken symmetry from Section 6.2. The condition numbers of the Jacobian were very similar. Let's therefore focus on the speed. The continuation which makes SParam1 zero took 11.8 seconds with the Riccati equations and 10.9 seconds with the method of Beyn et al. [2001]. To find the zero of SParam2 17.9 seconds were needed in our approach against 20.2 in the approach of Beyn et al. [2001]. The third homotopy step lasted 231.2 seconds against 244.2 seconds. And the continuation of 100 homoclinic orbits took 118.6 seconds when using the Riccati equations while it took 116.1 seconds when using the method proposed in Beyn et al. [2001]. Similar results were obtained in the other examples. Therefore, we can conclude that for relatively low-dimensional ODEs both methods are comparable in speed and robustness and the condition number of the Jacobian is of the same order. Further tests are required to compare the methods in higher dimensions.

The current version of MATCONT does support the initialization of the saddle homoclinic orbit from a Bogdanov-Takens equilibrium point, that is a local bifurcation of codim 2, see Beyn et al. [2002] for the implemented algorithm. Homoclinic orbits are also known to bifurcate from other codim 2 equilibria, at fold-Hopf and double Hopf bifurcations (see Guckenheimer and Holmes [1983] and Kuznetsov [2004] and references therein). The initialization of such homoclinic orbits in MATCONT is a work in progress that will be reported elsewhere.

In this article we have described new features of MATCONT concerning orbits connecting equilibria. We have introduced a defining BVP for the continuation of such orbits, in which the Riccati equations used to set up the projection boundary conditions are explicitly included. Furthermore, we have extensively discussed a

homotopy method for the initialization of homoclinic and heteroclinic orbits. We have given the algorithm in detail in the case of HHS orbits, and described the differences of the method in the HSN case and the case of heteroclinic orbits. Numerous examples have illustrated the method. We have given an overview of the test functions for all codimension-two homoclinic bifurcations and paid special attention to the inclination-flip case, for which a better method is proposed and implemented. All described algorithms are interactively supported in MATCONT, which makes it – together with the earlier implemented features – a unique research environment.

APPENDIX: Homotopy Method for Heteroclinic Orbits

ALGORITHM 3. Locating a Heteroclinic Orbit by Homotopy.

Input.

$x_0^{(0)} \in \mathbb{R}^n$, $x_1^{(0)} \in \mathbb{R}^n$, $\alpha = (\alpha_1, \ldots, \alpha_{n_\alpha - 1}) \in \mathbb{R}^{n_\alpha - 1}$, $f_x(x_0^{(0)}, \alpha)$, $f_x(x_1^{(0)}, \alpha)$, and the real Schur factorizations of these matrices.

(1) **Locating a connecting orbit, α is fixed.**
Step 1. The first step can be done either by time integration or by continuation. If we choose time integration, we start from $x(0) = x_0^{(0)} + \epsilon_0(c_1 q_{0,1}^{(0)} + c_2 q_{0,2}^{(0)})$, with the same remark about c_1 and c_2 as for HHS orbits. If continuation is used, we set $x(t) = x_0^{(0)} + \epsilon_0(c_1 q_{0,1}^{(0)} + c_2 q_{0,2}^{(0)})$ in $[0, T]$ for a small value of T and ϵ_0, and extend this segment by continuation using the following equations:

$$
\begin{aligned}
&\dot{x}_C - 2Tf(x_C, \alpha) = 0,\\
&\epsilon_0 c_i - \langle x(0) - x_0^{(0)}, q_{0,i}^{(0)} \rangle = 0, \quad i = 1, ..., n_U,\\
&\tau_i - \tfrac{1}{\epsilon_1} \langle x(1) - x_1^{(0)}, q_{1,n_S+i}^{(0)} \rangle = 0, \quad i = 1, ..., n - n_S,\\
&\langle x(0) - x_0^{(0)}, q_{0,n_U+i}^{(0)} \rangle = 0, \quad i = 1, ..., n - n_U,\\
&\|x(1) - x_1^{(0)}\| - \epsilon_1 = 0.
\end{aligned}
$$

This gives us $n_c = Nmn + 2n - n_S + 1$ constraints and the free scalar variables are $x_M, \tau_1, \ldots \tau_{n-n_S}, T, \epsilon_1$ so that $n_v = Nmn + 2n - n_S + 2$.
We stop the time integration or continuation when ϵ_1 stops decreasing.
Steps k, $k = 2, ..., n_U$ (for $n_U > 1$). Compute a branch of solutions to the system

$$
\begin{aligned}
&\dot{x}_C - 2Tf(x_C, \alpha) = 0,\\
&\epsilon_0 c_i - \langle x(0) - x_0^{(0)}, q_{0,i}^{(0)} \rangle = 0, \quad i = 1, ..., n_U,\\
&\tau_i - \tfrac{1}{\epsilon_1} \langle x(1) - x_1^{(0)}, q_{1,n_S+i}^{(0)} \rangle = 0, \quad i = 1, ..., n - n_S,\\
&\langle x(0) - x_0^{(0)}, q_{0,n_U+i}^{(0)} \rangle = 0, \quad i = 1, ..., n - n_U,\\
&\|x(0) - x_0^{(0)}\| - \epsilon_0 = 0,\\
&\|x(1) - x_1^{(0)}\| - \epsilon_1 = 0,
\end{aligned}
$$

to locate a zero of, say, τ_{k-1} (while $\tau_1, \ldots, \tau_{k-2} = 0$, fixed). The number of constraints is $n_c = Nmn + 2n - n_S + 2$ and the free scalar variables are given by $x_M, c_1, \ldots c_k, \tau_{k-1}, \ldots \tau_{n-n_S}, \epsilon_1$ so that $n_v = Nmn + 2n - n_S + 3$, and thus $n_c - n_v = -1$.
At the end of these successive continuations $\tau_1 = \ldots = \tau_{n_U - 1} = 0$. Remark that the τ's can be made zero in any possible order.

(2) **Locating a connecting orbit, α varies**.
Steps k, $k = n_U + 1, ..., n - n_S + 1$ (for $n - n_S \geq n_U$). Compute a branch of solutions to the system

$$\begin{aligned}
&\dot{x}_C - 2Tf(x_C, \alpha) = 0,\\
&f(x_0, \alpha) = 0,\\
&f(x_1, \alpha) = 0,\\
&\langle x(0) - x_0, q_{0,n_U+i}\rangle = 0, \quad i = 1, ..., n - n_U,\\
&\tau_i - \tfrac{1}{\epsilon_1}\langle x(1) - x_1, q_{1,n_S+i}\rangle = 0, \quad i = 1, ..., n - n_S,\\
&T_{22U}Y_U - Y_U T_{11U} + T_{21U} - Y_U T_{12U} Y_U = 0,\\
&T_{22S}Y_S - Y_S T_{11S} + T_{21S} - Y_S T_{12S} Y_S = 0,\\
&\left\|x(0) - x_0\right\| - \epsilon_0 = 0,\\
&\left\|x(1) - x_1\right\| - \epsilon_1 = 0,
\end{aligned}$$

where $Y_U \in \mathbb{R}^{(n-n_U)\times n_U}$, $Y_S \in \mathbb{R}^{(n-n_S)\times n_S}$, to locate a zero of τ_{k-1} (while $\tau_1, ..., \tau_{k-2} = 0$, fixed). The number of constraints is $n_c = Nmn + 4n - n_U - n_S + 2 + (n - n_U)n_U + (n - n_S)n_S$ and the free scalar variables are $x_M, x_0, x_1, \alpha_1, \ldots, \alpha_{k-n_U}, \tau_{k-1}, \ldots, \tau_{n-n_S}, \epsilon_1, Y_U, Y_S$ so that $n_v = Nmn + 4n - n_U - n_S + 3 + (n - n_U)n_U + (n - n_S)n_S$.
At the end of these homotopies all the τ's are zero. Again, any order in which zero intercepts of the τ's are detected is possible.

(3) **Increasing the accuracy of the connecting orbit, α varies**.
Step $n - n_S + 2$. Compute a branch of solutions to the system

$$\begin{aligned}
&\dot{x}_C - 2Tf(x_C, \alpha) = 0,\\
&f(x_0, \alpha) = 0,\\
&f(x_1, \alpha) = 0,\\
&\langle x(0) - x_0, q_{0,n_U+i}\rangle = 0, \quad i = 1, ..., n - n_U,\\
&\langle x(1) - x_1, q_{1,n_S+i}\rangle = 0, \quad i = 1, ..., n - n_S,\\
&T_{22U}Y_U - Y_U T_{11U} + T_{21U} - Y_U T_{12U} Y_U = 0,\\
&T_{22S}Y_S - Y_S T_{11S} + T_{21S} - Y_S T_{12S} Y_S = 0,\\
&\left\|x(0) - x_0\right\| - \epsilon_0 = 0,\\
&\left\|x(1) - x_1\right\| - \epsilon_1 = 0,
\end{aligned}$$

where $Y_U \in \mathbb{R}^{(n-n_U)\times n_U}$, $Y_S \in \mathbb{R}^{(n-n_S)\times n_S}$, in the direction of decreasing ϵ_1 until this end distance is "small". The number of constraints is $n_c = Nmn+4n-n_U-n_S+2+(n-n_U)n_U+(n-n_S)n_S$ and the free scalar variables are $x_M, x_0, x_1, \alpha_1, \ldots, \alpha_{n_\alpha-1}, T, \epsilon_1, Y_U, Y_S$ so that $n_v = Nmn+3n+n_\alpha+1+(n-n_U)n_U+(n-n_S)n_S = Nmn+4n-n_U-n_S+3+(n-n_U)n_U+(n-n_S)n_S$.

After these homotopies, a proper starting orbit for the continuation of heteroclinic orbits is obtained.

ACKNOWLEDGMENTS

The authors would like to thank the referees for their comments, which have led to a substantial improvement in the presentation of the article.

REFERENCES

BERESTYCKI, H. AND NIRENBERG, L. 1992. Travelling fronts in cylinders. *Ann. Inst. H. Poincaré Anal. Non Linéaire 9,* 5.

BEYN, W. J. 1990. The numerical computation of connecting orbits in dynamical systems. *IMA J. Numer. Anal. 10,* 3, 379–405.

BEYN, W. J., KLESS, W., AND THÜMMLER, V. 2001. Continuation of low-dimensional invariant subspaces in dynamical systems of large dimension. In *Ergodic Theory, Analysis, and Efficient Simulation of Dynamical Systems*, B. Fiedler Ed. Springer, Berlin, 47–72.

BEYN, W. J., CHAMPNEYS, A., DOEDEL, E., GOVAERTS, W., KUZNETSOV, YU. A., AND SANDSTEDE, B. 2002. Numerical continuation, and computation of normal forms. In *Handbook of Dynamical Systems*, B. Fiedler Ed., Vol. 2. Elsevier Science, North Holland, Amsterdam, 149–219.

BINDEL, D., DEMMEL, J., AND FRIEDMAN, M. 2008. Continuation of invariant subspaces in large scale bifurcation problems. *SIAM J. Sci. Comput. 30,* 2, 637–656.

BYKOV, V. V. 1978. On the structure of a neighborhood of a separatrix contour with a saddle-focus. In *Methods of Qualitative Theory of Differential Equations*, Gorkii State University, Gorkii, 3–32 (In Russian).

BYKOV, V. V. 1980. Bifurcations of dynamical systems close to systems with a separatrix contour containing a saddle-focus. In *Methods of Qualitative Theory of Differential Equations*, Gorkii State University, Gorkii, 44–72 (In Russian).

CHAMPNEYS, A. R. AND KUZNETSOV, YU. A. 1994. Numerical detection and continuation of codimension-two homoclinic bifurcations. *Int. J. Bifur. Chaos Appl. Sci. Eng. 4,* 4, 785–822.

CHAMPNEYS, A. R., KUZNETSOV, YU. A., AND SANDSTEDE, B. 1996. A numerical toolbox for homoclinic bifurcation analysis. *Int. J. Bifur. Chaos Appl. Sci. Eng. 6,* 5, 867–887.

DEMMEL, J. W., DIECI, L., AND FRIEDMAN, M. J. 2000. Computing connecting orbits via an improved algorithm for continuing invariant subspaces. *SIAM J. Sci. Comput. 22,* 1, 81–94.

DHOOGE, A., GOVAERTS, W., AND KUZNETSOV, YU. A. 2003. MATCONT: A MATLAB package for numerical bifurcation analysis of ODEs. *ACM Trans. Math. Softw. 29,* 2, 141–164.

DIECI, L. AND EIROLA, T. 1999. On smooth decompositions of matrices. *SIAM J. Matrix Anal. Appl. 20,* 3, 800–819.

DIECI, L. AND FRIEDMAN, M. J. 2001. Continuation of invariant subspaces. *Numer. Linear Algebra Appl. 8,* 5, 317–327.

DOEDEL, E. J. AND FRIEDMAN, M. J. 1989. Numerical computation of heteroclinic orbits. *J. Comput. Appl. Math. 26,* 1–2, 155–170.

DOEDEL, E. J., FRIEDMAN, M. J., AND MONTEIRO, A. C. 1994. On locating connecting orbits. *Appl. Math. Comput. 65,* 1–3, 231–239.

DOEDEL, E. J., CHAMPNEYS, A. R., FAIRGRIEVE, T. F., KUZNETSOV, YU. A., SANDSTEDE, B., AND WANG, X.-J. 1997a. AUTO97: Continuation and bifurcation software for ordinary differential equations (with HomCont). http://indy.cs.concordia.ca/auto.

DOEDEL, E. J., FRIEDMAN, M. J., AND KUNIN, B. I. 1997b. Successive continuation for locating connecting orbits. *Numer. Algor. 14,* 1-3, 103–124.

FRIEDMAN, M., GOVAERTS, W., KUZNETSOV, YU. A., AND SAUTOIS, B. 2005. Continuation of homoclinic orbits in MATLAB. In *Proceedings of the 5th International Conference on Computational Science*, V. S. et al. Ed. Springer Verlag Lecture Notes in Computer Science Series, vol. 3514, ICCS, Atlanta, GA, 263–270.

GHAZIANI, R. K., GOVAERTS, W., KUZNETSOV, YU. A., AND MEIJER, H. G. E. 2009. Numerical continuation of connecting orbits of maps in matlab. *J. Diff. Equ. Appl. 15,* 8–9, 849–875.

GLENDINNING, P. AND SPARROW, C. 1986. T-points: A codimension two heteroclinic bifurcation. *J. Stat. Phys. 43,* 3–4, 479–488.

GOVAERTS, W. 2000. *Numerical Methods for Bifurcations of Dynamical Equilibria*. SIAM, Philadelphia, PA.

GOVAERTS, W., DE WITTE, V., AND KHEIBARSHEKAN, L. 2009. Using MATCONT in a two-parameter bifurcation study of models for cell cycle controls. In *Proceedings of the ASME International Design Engineering Technical Conferences and Computers and Information in Engineering Conference*. IDETC/CIE, CA.

GRAY, P. AND SCOTT, S. K. 1990. *Chemical Oscillations and Instabilities: Non-linear Chemical Kinetics*. Oxford University Press, Oxford, UK.

GUCKENHEIMER, J. AND HOLMES, P. 1983. *Nonlinear Oscillations, Dynamical Systems and Bifurcations of Vector Fields*. Springer, New York.

KUZNETSOV, YU. A. 2004. *Elements of Applied Bifurcation Theory* 3rd Ed. Springer, New York.

KUZNETSOV, YU. A. AND LEVITIN, V. V. 1998. CONTENT: Integrated environment for analysis of dynamical systems, version 1.5. http://ftp.cwi.nl/CONTENT.

LORENZ, E. N. 1963. Deterministic nonperiodic flow. *J. Atmospher. Sci. 20,* 2, 130–141.

PETROVSKAYA, N. V. AND JUDOVICH, V. I. 1980. Homoclinic loops of the Salzman-Lorenz system. In *Methods of Qualitative Theory of Differential Equations*, Gorkii State University, Gorkii, 73–83 (In Russian).

RINZEL, J. AND ERMENTROUT, G. B. 1989. Analysis of neural excitability and oscillations. In *Methods in Neuronal Modeling: From Synapses to Networks*, C. Koch and I. Segev Eds., MIT Press, Cambridge, MA, 135–169.

TYSON, J. J. AND NOVAK, B. 2001. Regulation of the eukaryotic cell cycle: Molecular antagonism, hysteresis, and irreversible transitions. *J. Theor. Biol. 210,* 2, 249–263.

Received June 2010; revised February 2011 and September 2011; September 2011